EFFECTS OF NANOSCALE ZERO-VALENT IRON (NZVI) ON BACTERIAL VIABILITY: ROLES OF GROWTH PHASES AND OXIDATIVE STRESS

A Thesis
Submitted to the Graduate Faculty
of the
North Dakota State University
of Agriculture and Applied Science

By

Krittanut Chaithawiwat

In Partial Fulfillment of the Requirements
for the Degree of
MASTER OF SCIENCE

Major Program:
Environmental and Conservation Sciences

April 2011

Fargo, North Dakota

North Dakota State University
Graduate School

Title

EFFECTS OF NANOSCALE ZERO-VALENT IRON (NZVI) ON BACTERIAL SURVIVABILITY: ROLES OF GROWTH PHASES AND OXIDATIVE STRESS

By

Krittanut Chaithawiwat

The Supervisory Committee certifies that this ***disquisition*** complies with North Dakota State University's regulations and meets the accepted standards for the degree of

MASTER OF SCIENCE

ABSTRACT

Chaithawiwat, Krittanut, M.S., Environmental and Conservation Science Program, College of Graduate and Interdisciplinary Studies, North Dakota State University, April 2011. Effects of Nanoscale Zero-valent iron (nZVI) on Bacterial Viability: Roles of Growth Phases and Oxidative Stress. Major Professors: Drs. Eakalak Khan and John McEvoy.

The effect of nanoscale zero-valent iron (nZVI) particles on bacteria from different growth phases was studied. Four bacterial strains including *Escherichia coli* strains JM109 and BW25113, and *Pseudomonas putida* strains KT2440 and F1 were experimented. The growth characteristics of these strains were determined. Their cells were harvested based on predetermined time points corresponding to different growth phases and exposed to nZVI. The cell viability was determined by a plate count method. The cells in lag and stationary phases showed higher resistance to nZVI for all four bacterial strains, whereas the cells in exponential and decline phases were less resistant and were rapidly inactivated when exposed to nZVI. Bacterial inactivation increased with the concentration of nZVI. Furthermore, less than 14% reduction in viability was observed when the cells were exposed to the leachate of nZVI suspension suggesting that the physical interaction between nZVI and the cells is critical for bacterial inactivation.

To understand the physiology that underlines these phenotypes, the responses from various oxidative stress gene knockout strains of *E. coli* BW25113 to nZVI were examined. For each of these mutant strains, cells from different growth phases were collected and exposed to nZVI. The viability of the cells was determined by a plate count method. All of the mutant strains exhibited higher susceptibility to nZVI when compared to the wild type strain. The results also indicated that different knockout strains exhibited different levels of susceptibility to nZVI. Strain lacking RpoS, a global stress regulator, showed the highest

susceptibility. Among different defensive enzyme mutants, *sodA* and *sodB* mutants exhibited the highest vulnerability whereas *sodC* mutant revealed much less susceptibility, suggesting that nZVI may induce oxidative stress inside the cells via superoxide generation. The inducibility of catalase (hydroperoxidase I) was also investigated by exposing the cells to nZVI and measuring a related gene expression using quantitative polymerase chain reaction. Results suggested that nZVI repressed the expression of this enzyme.

ACKNOWLEDGEMENTS

I would like to gratefully thank my advisors, Drs. Eakalak Khan and John McEvoy, for their guidance and support, and for accepting me as their student. I also would like to express my appreciation to Dr. Alisa Vangnai for her support and encouragement. Without any of them, this work would not be completed. I also would like to acknowledge Dr. Birgit Pruess for her help and suggestions. I also appreciate Dr. Glenn Dorsam for opening my world in molecular biology through his Bioc 719 course and for being my committee member.

I would like to extend my acknowledgements and appreciation to those in Dr. McEvoy's laboratory, including Cathy Giddings, Ebot Tabe, Brianna Schneck, and Tu Le for their assistance and encouragement throughout my study. My appreciation is also extended to Curt Doetkott for his assistance in statistical analysis, Sita Krajangpan for zero valent nanoparticles preparation, my parents and Piangpinit Kammaruckampol for their endless support and belief. Finally, I would like to thank my friends and family whom I did not name here for their sincere support throughout my study.

TABLE OF CONTENTS

LIST OF TABLES

LIST OF FIGURES

CHAPTER 1. INTRODUCTION

1.1 Background

The capability to manipulate matters in the nanoscale or nanotechnology has been tremendously developed, improved, and explored during the last few decades. Novel applications of nanomaterial and nanoparticles related to construction, electronic devices, industrial catalysts, drug carriers, and medical diagnosis have been widely populated (Huber, 2005). Among different types of available nanoparticles, iron nanoparticles especially nanoscale zero valent iron (nZVI) are one of most promising materials for environmental applications, due to their ability to transform, detoxify, or degrade various commonly found contaminants in the environment and hazardous waste sites (Theron et al., 2008; Liu et al., 2005; Grieger et al., 2010). It has been shown that nZVI particles exhibit much higher reactivity compared to their microscale zero-valent iron (ZVI) counterpart due to their high specific surface area per volume (Wang and Zhang, 1997). Hazardous substance transformation using nZVI can be accomplished in a short period of time both in situ and ex situ (Li et al., 2006; Zhang, 2003; Grieger et al., 2010). This leads to an inevitably direct release of nZVI into environment which raises concerns about its toxic potential (Grieger et al., 2010; Barnes et al., 2010).

Several studies suggested that nanoparticles including nZVI are toxic to cells and living organisms, mainly due to their size and potential to generate reactive oxygen species (ROS) such as superoxide, hydrogen peroxide, and hydroxyl radical (Nel et al., 2006; Keenan et al., 2009; Diao and Yao, 2009). A limited level of ROS is naturally generated in aerobically growing cells as oxygen by-products resulting from the electron transport chain

(Lushchak, 2001). Since ROS can rapidly react with cell components such as protein, lipid, and nucleic acid [deoxyribonucleic acid (DNA) and ribonucleic acid (RNA)], causing damage to these components, mitigation of these ROS is necessary in both prokaryotic and eukaryotic cells (Storz, Tartaglia, Farr et al., 1990; Lushchak, 2001). General strategies for protecting cell from ROS includes reducing ROS metabolite, protecting cell components against ROS, and repairing damages caused by ROS (Lushchak, 2001).

1.2 Research Justification

Due to increasing concerns regarding the toxicity of nanoparticles, research has been conducted in order to elucidate their toxic potential (Nel et al., 2006). Bacteria were used as a model organism in several previous studies to evaluate the toxicity of nanomaterials (Lee et al., 2008; Diao and Yao, 2009; Auffan et al., 2008), and most if not all of these bacterial cells were from stationary phase, which is only one phase of the bacterial growth. The physiological characteristics of bacterial cells in different growth phases can be very different, and may provide different responses to the challenge of possible toxic substances (Eisenstark et al., 1996; Dong et al., 2008). For example, bacterial cells from different growth phases exhibit different resistance toward oxidative stress introduced by neutrophils (Bortolussi et al., 1987).

The aim of this research is to determine the effect of nZVI on bacterial cells in different growth phases to see if different responses can be observed. A previous study suggested that oxidative stress induced by ROS is responsible for cell inactivation (Nel et al., 2006). In the case of nZVI, all related research so far proposed that ROS also contribute to cell inactivation (Lee et al., 2008; Keenan et al., 2009; Diao and Yao, 2009; Auffan et al., 2008). However, the mechanism in which these ROS damage cell has not been clearly

elucidated. Thus this research also intends to examine the molecular responses of bacteria to nZVI by using oxidative stress related mutants from various growth phases and measuring the expression of oxidative stress related genes in order to gain greater insight into inactivation mechanism of nZVI.

1.3 Objectives

1. To study the toxic effects of nanoscale zero-valent iron particles (nZVI) on bacterial cells in different growth phases.
2. To investigate the role of oxidative stress responses in bacterial inactivation by nZVI.

1.4 Hypotheses

1. Bacterial cells in different growth phases exhibit different responses toward nZVI.
2. Oxidative stress induced by nZVI contributes to bacterial inactivation.

1.5 Thesis Organization

This thesis consists of 5 chapters. The first chapter (This chapter), which is the introduction, includes research background and justification, objectives, and hypotheses. Literature review is presented in Chapter 2. Chapters 3 and 4, entitled "Effects of nanoscale zero-valent iron particles on bacterial survivability: role of growth phases" and "Role of oxidative stress in bacterial inactivation by nanoscale zero-valent iron (nZVI)", are work corresponding to the objectives of the study and will be modified and submitted for journal publications in the near future. Conclusions and recommendations for future studies are provided in Chapter 5.

CHAPTER 2. LITERATURE REVIEW

2.1 Nanoscale Zero-valent Iron Particles

Nanoparticles are defined as extremely small particle in which at least one dimension is smaller than 100 nm (Nel et al., 2006). nZVI particles are the nanoscale particle form of zero-valent iron, which exhibit significantly higher reactivity compared to their microscopic counterpart (Wang and Zhang, 1997). The high reactivity of these particles comes from their high surface area ratio per volume which allows more reactions to occur at the same time (Nurmi et al., 2004). Also when the particle size decreases, the surface atoms become less stable due to high surface energy which is resulted from increased proportion between surface and near surface atoms. Therefore high energy atoms at the surface of the particle tend to interact rapidly with other nearby molecules in order to stabilize the high surface energy (Li et al., 2006; Zhang, 2003). Furthermore, another less reactive metal such as Pd, Ni, Pt, or Ag can be added on nZVI surface forming bimetallic particles which have even higher reactivity (Theron et al., 2008; Zhang, 2003).

2.1.1 Structure of nZVI

nZVI typically exhibits a core-shell structure consisting of a zero-valent iron core and a mixed valent oxide layer outside the core. Figure 2.1a presents a theoretical structure of this core-shell nZVI, and nZVI under transmission electron microscope (TEM) is shown in Figure 2.1b. The oxide layer is generated from the oxidation of iron at the particle surface forming a mixed-valent of ferrous and ferric oxide (Li et al., 2006). The shell compositions of nZVI are also affected by the size of particles (Signorini et al., 2003). Although nZVI may exhibit some of their iron oxide properties, the overall properties of

the particles are based on both shell and core parts (Nurmi et al., 2004). Many applications of nZVI are based on the electron donating property of these particles which involves the electrons donated from zero-valent iron core of the particles (Liu et al., 2005). Due to their colloidal nature, nZVI have high tendency to agglomerate forming a larger size of particles leading to their lower reactivity due to the reduced specific surface area per volume (Phenrat et al., 2006). nZVI also exhibits strong binding to natural materials such as soil which can limit the migration of these particles toward the target zone of remediation (Schrick et al., 2004). Several studies have aimed to reduce this agglomeration and binding effects of nZVI in order to increase the efficiency of these particles (Nurmi et al., 2004; Phenrat et al., 2006; Theron et al., 2008).

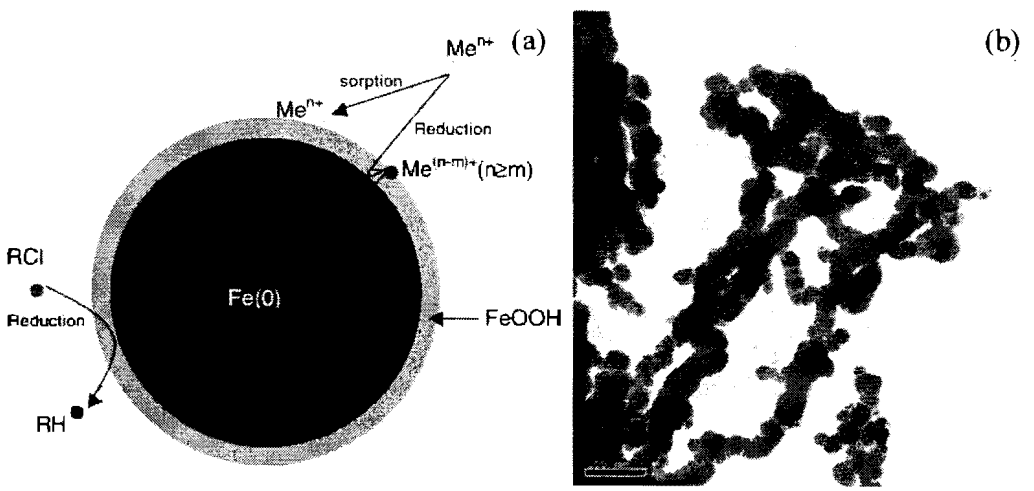

Figure 2.1: (a) Conceptual core-shell structure of nZVI (Li et al., 2006), and (b) nZVI under TEM (Zhang and Elliott, 2006)

2.1.2 Synthesis and characterization of nZVI

There are two main approaches for nZVI synthesis: top-down and bottom-up approaches. The top-down approach involves generating small particles by reducing the

size of large material using mechanical and/or chemical processes such as milling and machining, whereas the latter approach focuses on growing the iron particle atom by atom on supporting surface via chemical reactions (Li et al., 2006). nZVI was successfully synthesized using both strategies; however, most studies fabricated nZVI using reduction of ferrous or ferric to zero-valent iron with sodium borohydride due to the simplicity of the synthesis, which requires only limited reagents and instruments (Li et al., 2006; Sun et al., 2006; Liu et al., 2005; Wang and Zhang, 1997). In case of bimetallic iron nanoparticles, the newly synthesized nZVI was immersed in the solution of the second metal salt (Li et al., 2006).

2.2. Application of nZVI

nZVI has been intensively used in toxic substance transformation due to their high reactivity (Zhang, 2003). Microscale zero-valent iron (ZVI) particles were first used for environmental remediation in 1994 (Grieger et al., 2010). They were applied into permeable reactive barriers for groundwater cleanup. Subsequently, they were used in many cleanup efforts throughout America, Europe, and Asia (Li et al., 2006). Although not all of the nanoparticles would enhance reactivity compared to their microscopic counterpart, research has indicated significantly higher reactivity of nZVI over the microscale iron particles for contaminant remediation (Wang and Zhang, 1997). Wang and Zhang (1997) compared the transformation of 20 mg/L of trichloroethene (TCE) using synthesized nZVI, ZVI, and microscopic Pd/Fe particles. Among these particles, nZVI exhibited the highest transformation rate, and achieved complete dehalogenation in 1.7 hour. Degradation of lindane, which was one of the most used chlorinated organic

pesticides, by nZVI and ZVI was studied (Li et al., 2006). At an initial lindane concentration of 700 μg/L, 95% of lindane was degraded by 2.2 to 27 g/L of nZVI within 48 hours while only 41% was degraded by ZVI.

For many of the organic contaminants which contain halogen atom in their molecule such as chlorinated organic solvent, chlorinated organic pesticide, polychlorinated biphenyls, and organic dye can be effectively dehalogenated by the electrons provided by zero-valent iron as indicated in equations [2.1],[2.2], and [2.3] (Li et al., 2006). In equation [2.1] zero-valent iron serves as a source of electrons. Then, the released free electrons from zero-valent iron are transferred to halogenated compound as shown in equation [2.2]. Finally, the combined reaction is presented in equation [2.3].

$$Fe^0 \rightarrow Fe^{2+} + 2e^- \qquad [2.1]$$

$$RCl + H^+ + 2e^- \rightarrow RH + Cl^- \qquad [2.2]$$

$$RCl + Fe^0 + H^+ \rightarrow RH + Fe^{2+} + Cl^- \qquad [2.3]$$

Ferrous iron at the shell of nZVI can also reduce the halogenated contaminant; however, at a much slower rate compared to its zero-valent form. According to this contaminant reduction process, the toxicity of the contaminant is also expected to decrease since, in most cases, the toxicity depends on the number of halogen in the molecule (Li et al., 2006). Studies have shown that nZVI are an effective solution to many persistent contaminants including, but not limited to, perchloroethene, TCE, carbon tetrachloride, organic pesticide such as dichlorodiphenyltrichloro-ethane, and a wide variety of halogenated solvents, which are commonly detected in hazardous waste sites (Liu et al.,

2005; Chang and Kang, 2009; Grieger et al., 2010). More of these common contaminants are shown in Table 2.1.

The efficiency of nZVI in term of contaminant transformation was evaluated via both laboratory experiments and field demonstrations (Liu et al., 2005; Quinn et al., 2005; Grieger et al., 2010). For example, one of the laboratory studies was conducted with groundwater sample containing 6070 μg/L of trichloroethane, 4680 μg/L of TCE, and small amounts of some other chlorinated hydrocarbons. Ninety nine percent dechlorination of all contaminants was obtained within 24 hours (Zhang, 2003). In terms of field demonstration, in situ remediation of TCE using nZVI was successfully demonstrated. About 14000 μg/L of TCE was detected before the injection of slurry form of nZVI into the groundwater, and the subsequent concentration of TCE was monitored at the injection well and monitoring well located 7.5 m from the injection well. Ninety percent of TCE at the injected site was rapidly dechlorinated within a few days after the injection, and 68% of TCE at the monitoring well was treated within 10 days and became undetectable in 50 days (Zhang, 2003).

2.3. Toxicity of nZVI

Despite the advance in nanotechnology and its increasing applications, concerns about potential environmental and health hazard from these novel nanoparticles have been raised (Nel et al., 2006; Grieger et al., 2010). Research has been conducted in order to elucidate these concerns, and recent studies have shown that many of these nanoparticles

Table 2.1: Common contaminants that can be transformed by nZVI(Zhang, 2003)

Chlorinated methanes	Trihalomethanes
Carbon tetrachloride (CCl_4)	Bromoform ($CHBr_3$)
Chloroform ($CHCl_3$)	Dibromochloromethane ($CHBr_2Cl$)
Dichloromethane (CH_2Cl_2)	Dichlorobromomethane ($CHBrCl_2$)
Chloromethane (CH_3Cl)	Chlorinated ethenes
Chlorinated benzenes	Tetrachloroethene (C_2Cl_4)
Hexachlorobenzene (C_6Cl_6)	Trichloroethene (C_2HCl_3)
Pentachlorobenzene (C_6HCl_5)	*cis*-Dichloroethene ($C_2H_2Cl_2$)
Tetrachlorobenzenes ($C_6H_2Cl_4$)	*trans*-Dichloroethene ($C_2H_2Cl_2$)
Trichlorobenzenes ($C_6H_3Cl_3$)	1,1-Dichloroethene ($C_2H_2Cl_2$)
Dichlorobenzenes ($C_6H_4Cl_2$)	Vinyl chloride (C_2H_3Cl)
Chlorobenzene (C_6H_5Cl)	Other polychlorinated hydrocarbons
Pesticides	PCBs
DDT ($C_{14}H_9Cl_5$)	Dioxins
Lindane ($C_6H_6Cl_6$)	Pentachlorophenol (C_6HCl_5O)
Organic dyes	Other organic contaminants
Orange II ($C_{16}H_{11}N_2NaO_4S$)	N-nitrosodimethylamine (NDMA) ($C_4H_{10}N_2O$)
Chrysoidine ($C_{12}H_{13}ClN_4$)	TNT ($C_7H_5N_3O_6$)
Tropaeolin O ($C_{12}H_9N_2NaO_5S$)	Inorganic anions
Acid Orange	Dichromate ($Cr_2O_7^{2-}$)
Acid Red	Arsenic (AsO_4^{3-})
Heavy metal ions	Perchlorate (ClO_4^-)
Mercury (Hg^{2+})	Nitrate (NO_3^-)
Nickel (Ni^{2+})	
Silver (Ag^+)	
Cadmium (Cd^{2-})	

can post adverse effects to living organisms including both eukaryotic cells and prokaryotic cells (Nel et al., 2006; Auffan et al., 2008; Diao and Yao, 2009). It has been shown that exposure to high concentrations of metal nanoparticles may induce lung inflammation and cause damages to several internal organs (Nel et al., 2006).

In the case of nZVI, several studies indicated adverse effects of nZVI toward human lung and bacterial cells (Auffan et al., 2008; Diao and Yao, 2009; Keenan et al., 2009; Lee et al., 2008). In a study by Lee et al. (2008), the toxicity of nZVI on *Escherichia coli* under aerobic and anaerobic conditions was tested. The results indicated a high inactivation rate of *E. coli* under anaerobic condition, while a much lower inactivation rate was observed under aerobic condition. Interestingly, the addition of hydroxyl radical

scavenger under aerobic condition showed no effect to the toxicity of nZVI suggesting that hydroxyl radical might not significantly contribute to the observed toxic effect. It was also proposed that cell membrane disruption may contribute to inactivation mechanism due to the interaction between iron particles and functional groups of proteins and lipopolysaccharide of cell membrane.

Auffan et al. (2008) also observed a toxic effect of nZVI on *E. coli* under experimental conditions. Furthermore, absolute inactivation (100%±20%) of *E. coli* lacking a cytolosic superoxide dismutase, which is encoded by *sodA* and *sodB*, was observed suggesting that superoxide dismutase is involved in protecting bacterial cells against nZVI. Toxicity of nZVI on Gram positive bacteria and fungi was examined by Giao and Yao (2009). Gram positive bacteria (*Bacillus subtilis*) exhibited higher resistance to nZVI when compared to Gram negative bacteria (*Pseudomonas fluorescens*), and no toxic effect was found in fungi (*Aspergillus versicolor*), suggesting that different membrane components may affect the toxicity of nZVI. The inactivation mechanism in which nZVI induces oxidative stress and interferes membrane function was proposed.

Effects of nZVI on mammalian cells were examined by Keenan et al. (2009) through the exposure of nZVI to human bronchial cells. The results indicated the toxic effect of nZVI on the cells, and that the toxicity was correlated with the dosage of particles used. Similar to the results of Lee et al. (2008), no significant generation of hydroxyl radical was detectable using benzoate, which usually rapidly reacts with hydroxyl radical, indicating that hydroxyl radical may not responsible for cell inactivation. These studies proposed that major mechanisms, which are responsible for living cells inactivation,

include induction of oxidative stress, cell membrane damage or disruption, and disturbance of intracellular functions. A summary of some of the recent studies is shown in Table 2.2. The presence of nZVI in rivers may affect the bacterial community in the environment and cause reduction of redox potential (Barnes et al., 2010).

2.4. Bacterial Growth Phases

Bacterial growth can be divided into 4 main phases namely lag phase, log or exponential phase, stationary phase, and death or decline phase as shown in Figure 2.2. In typical batch cultivation, bacteria enter lag phase once they are transferred into a fresh medium. During this phase, no increase of bacterial cells is observed since bacteria require time to adjust to the new environment by synthesizing necessary proteins for new growing condition and nutrient. The time required in this phase is significantly dependent on the media composition and growing condition. When cells are adapted to the new environment, they proceed to exponential phase in which rapid increase of cell number occurs due to binary fission of bacterial cells. However, when available nutrient and oxygen are almost depleted, together with accumulation of toxic metabolite, the growth of bacterial cells becomes steady, and cell enters stationary phase. Eventually, in death phase, when more toxic by-products of cell metabolism accumulate and nutrient is completely depleted, the number of viable cell decreases (White, 2007; Hogg, 2005). Bacteria express different physiological characteristics based on each growth phase. For example, certain enzymes are only synthesized in particular phases (Rahman et al., 2008; Miksch and Dobrowolski, 1995). Bacterial cells also respond differently to stress and antibiotics according to their growth phase (Ishihama, 1997; Kim and Anthony, 1981).

Table 2.2: Summary of nZVI toxicity related studies

	Auffan et al. (2008)	**Lee et al. (2008)**	**Keenan et al. (2009)**	**Diao and Yao (2010)**
nZVI synthesis	Reduction of ferrous sulfate using sodium borohydride	Reduction of ferric chloride using sodium borohydride	Reduction of ferrous sulfate using sodium borohydride	Reduction of ferric nitrate using sodium borohydride
nZVI size	320 ± 30 nm	10-80 nm	Not available	20-30 nm
nZVI concentration	7-700 mg/L	1.2-110 mg/L	50-250 μM Fe	100-10000 mg/L
Target cell	*Escherichia coli*	*Escherichia coli*	Human bronchial epithelial cell	*Bacillus subtilis*, *Pseudomonas fluorescens*, and *Aspergillus versicolor*
Inactivation time	1 hour	Up to 1 hour	1 hour	5 min
Inactivation rate	25-90%	> 99%	10-100%	80-100% for *B. subtilis*, 100% for *P. fluorescens*, and no effect on *A. versicolor*
Proposed inactivation mechanism	Oxidative stress, bacterial metabolism interfering	Oxidative stress, cell membrane disruption, and enzymatic function interfering	Oxidative stress	Oxidative stress and membrane function interfering

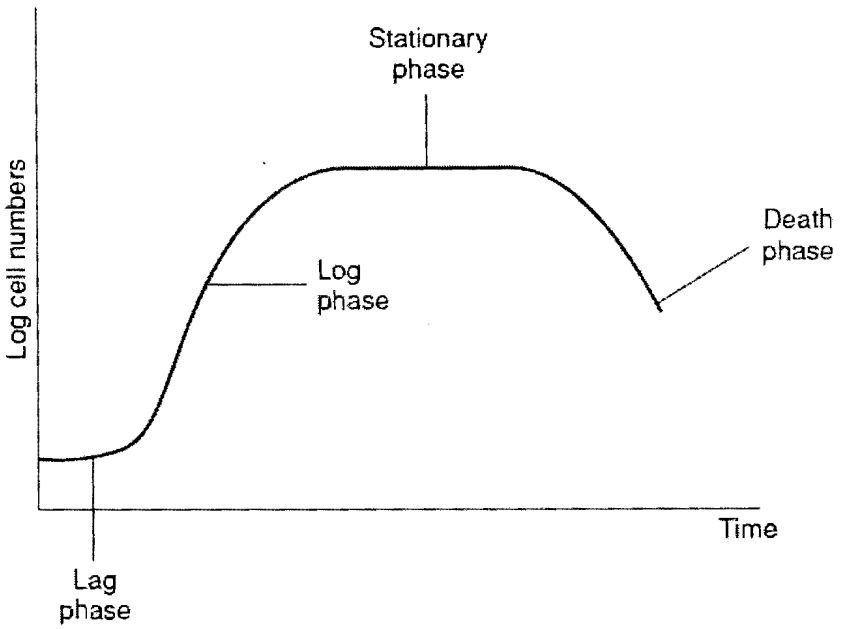

Figure 2.2: Typical growth curve of bacteria (Hogg, 2005)

Bacterial cells in different growth phases exhibit different physiological characteristics such as cellular metabolism and gene expression. This results in different cellular responses when these bacterial cells are challenged by stressful environment or toxic substances. Growth phase dependent acid resistance was found in *Listeria monocytogenes*, *Shigella flexneri*, *E. coli*, and *Salmonella* Typhimurium (Davis et al., 1996; Small et al., 1994; Lee et al., 1994). High resistance to acid stress was observed in stationary phase cells compared to cells cultured from exponential phase (Davis et al., 1996). Similarly, higher oxidative stress resistance was also observed in stationary phase cells compared to exponential phase cells (Vattanaviboon and Mongkolsuk, 2001). Susceptibility toward bactericidal substance such as penicillin is also growth phase

dependent since the expression of penicillin receptor was found in only certain bacterial growth phases (Stevens et al., 1993).

2.5. Oxidative Stress

Oxidative stress refers to an imbalance condition of cell where intracellular ROS including superoxide, hydrogen peroxide, and hydroxyl radical, overcome the defensive capability available in the cell (González-Flecha and Demple, 1995; Lushchak, 2001). Naturally, these ROS are constitutively generated when cells undergoes aerobic respiration in which the oxygen is consumed as a final electron acceptor in the electron transport chain (Storz, Tartaglia, Farr et al., 1990). These ROS residues are highly reactive and have potential to react with cellular components such as enzymes, structural proteins, lipids, and nucleic acid (Lushchak, 2001). In prokaryotic organisms, which are a single cellular organism, these interactions are highly lethal, while in eukaryotic organisms such as human, oxidative stress can cause systematic inflammation or various diseases (Lee et al., 2008; Nel et al., 2006). As a consequence, living cells have to develop a cascade of defensive mechanisms in order to mitigate these adverse effects (Lushchak, 2011; Iuchi and Weiner, 1996; Storz, Tartaglia, Farr et al., 1990).

2.5.1 Cellular damages

Reactive by-products of oxygen resulting from aerobic respiration (Gonzalez-Flecha and Demple, 1997; Storz, Tartaglia, Farr et al., 1990) such as superoxide, hydrogen peroxide, and hydroxyl radical have the potential to damage intracellular components. These ROS can also be generated from various oxidative stress inducing reagents such as redox-cycling agent, menadione and paraquat. In enterobacteria and pathogenic bacteria,

these ROS may be introduced via various host defensive mechanisms including phagocytosis (Lynch and Kuramitsu, 2000). Intracellular targets of these ROS are proteins, lipid, DNA, and RNA. In case of lipid, which is a major component of all cellular membrane, polyunsaturated lipid can be directly targeted by ROS initiating lipid peroxidation. This peroxidation of lipid can significantly reduce the fluidity of cellular membrane, which can further affect membrane function and/or disrupt the membrane (Su et al., 2009).

Proteins are another target of ROS, and exposure toward ROS is known to severely alter amino acid in the protein molecule. This alternation occurs through various mechanisms including oxidation of thiol group and ring structure of many amino acids (Lushchak, 2001). Nucleic acid, which includes both DNA and RNA, is also a major target of ROS. Both nitrogenous bases and ribose sugar in nucleic acid can be targeted by ROS which results in double strand and single strand breaks in the nucleic acid molecule. These nucleic acid damages potentially lead to point mutation, prevent the replication of DNA, and might cause some unrecoverable damages to cell that eventually lead to cell death (Valko et al., 2004).

2.5.2 Oxidative stress related genes

There are enormous numbers of genes involved in oxidative stress in bacteria. Each of these genes, which can be categorized as follows: preventive activity, damage repair or response regulation. These genes serve as a part of a much larger and more sophisticated network of molecular responses toward oxidative stress (Eisenstark et al., 1996; Demple, 1991; Lushchak, 2001; Michan et al., 1999; Dong et al., 2008). This fine-tuned network

allows bacterial cells to react and survive under stressful condition. Several protective enzymes including superoxide dismutase, catalase, alkyl hydroperoxidereductase (*ahpCF*), glutathione oxidoreductase (*gor*), and non-specific DNA binding protein (*dps*), are responsible for protecting cell components against different reactive residues (Storz, Tartaglia, Farr et al., 1990; Lushchak, 2001). For instance, when superoxide anion, which is one of ROS that is constitutively produced in cell under aerobic respiration, are generated in the cells, there are two main defensive enzymes responsible for the detoxification of these ROS namely catalase and superoxide dismutase (Iuchi and Weiner, 1996). Firstly, superoxide anion can be transformed to hydrogen peroxide, which is another form of ROS, by superoxide dismutase as shown in equation [4], followed by detoxification of hydrogen peroxide by catalase, as indicated in equation [5]. The generated oxygen and water molecules are harmless to the cells.

$$2O^{\bullet-}_2 + 2H^+ \rightarrow H_2O_2 + O_2 \qquad [4]$$

$$2H_2O_2 \rightarrow 2H_2O + O_2 \qquad [5]$$

A simplified regulatory system of superoxide and catalase genes was shown in Figure 2.3. Beside the defensive mechanisms via several different enzymes, another mechanism against oxidative stress is damage repairing, specifically DNA repairing enzymes such as exonuclease III encoded from *xthA* since ROS is known to cause damage to DNA (Lushchak, 2001). These mechanisms have to work in concert in order to protect cell from oxidative stress. Therefore, the regulation of these mechanisms is crucial for cell survival. There are many regulatory genes such as *rpoS*, *oxyR*, *soxRS*, *arcAB*, *fnr*, and *fur* involving the gene control which is necessary to mitigate the damage caused by ROS (Touati, 2000; Storz, Tartaglia, Farr et al., 1990; Storz, Tartaglia and Ames, 1990;

Nunoshiba et al., 1992). Among these regulons, *rpoS* has been intensively studied since it contributes to not only oxidative stress responses, but also other stress responses such as high osmolarity, pH and temperature (Dong et al., 2008).

2.5.2.1 Genes encoded for defensive enzyme

2.5.2.1.1 Catalase genes

Catalase activity in *E. coli* is possessed by hydroperoxidase which exhibits both catalase and peroxidase activities. The role of catalase, together with peroxidase, is to prevent the accumulation of intracellular hydrogen peroxide residue (Schellhorn, 1995). The catalase activity is responsible for mitigating hydrogen peroxide forming non-toxic molecules of water and oxygen as shown in equation [5], whereas the peroxidase activity consumes hydrogen peroxide to oxidize intracellular reductant (Schellhorn, 1995). Two types of hydroperoxidase are found in *E. coli*, hydroperoxidase I (HP1) and hydroperoxidase II (HP2). These are encoded from *katG* and *katE* genes, respectively (Triggs-Raine and Loewen, 1987).

HP1 is inducible under exposure to sublethal concentrations of hydrogen peroxide (Christman et al., 1985). In vitro, 100 fold increased expression of HP1 was detected, while the increase of HP1 expression in vivo was much less (Christman et al., 1985). According to Schelhorn (1995), HP1 accounted for only a minor part of intracellular activity of catalase. While the transcription of *katG* is not directly dependent on aerobic condition, 10 fold increase in the expression of *katG* was observed in aerobically growing *E. coli* cells. This is due to the regulation of the *oxyR* regulon which is highly expressed under aerobic growth condition (Storz, Tartaglia and Ames, 1990). The structural gene for *katG* is located

at 89.2 min on the *E. coli* chromosome. The protein structure of HP1 consists of four identical subunits of 80 kDa protein (Triggs-Raine and Loewen, 1987), and has high structural similarity to other peroxidase enzymes (Schellhorn, 1995). HP1 was identified as one of 30 proteins which are inducible by hydrogen peroxide (Christman et al., 1985). Some of these proteins, including HP1, are under the regulation of *oxyR*. This gene is constitutively expressed when cells are grown aerobically, but remains inactive in terms of *katG* transcription until the presence of hydrogen peroxide.

OxyR senses the oxidative stress via its cysteine residue (cys-199), which can be oxidized by hydrogen peroxide. The oxidized form of OxyR undergoes a conformation change and up regulates the expression *katG* (Michan et al., 1999; Storz, Tartaglia and Ames, 1990). Furthermore, *katG* does not correspond to only OxyR as it is also regulated by another global regulator—RpoS. However, during exponential phase, the effect of RpoS is limited while OxyR serves as the main regulator for HPI expression (Schellhorn, 1995). This was supported by a study conducted by Michan et al. (1999) where *rpoS* and *oxyR* genes were knocked-out and simultaneous expression of *katG* was measured. The results clearly showed that, *katG* expression was completely diminished in *oxyR* knocked-out strain, whereas expression of *katG* remained in *rpoS* knocked-out strains.

Expression of HP2 was found to be growth phase dependent, and is high at late exponential phase and stationary phase. In contrast to HP1, the expression of HP2 is not directly inducible by hydrogen peroxide (Schellhorn, 1995). The high expression of HP2 is mainly from the regulation of RpoS, a significant global regulator of stress responses during stationary phase. While RpoS only moderately stimulates the expression of HP1, HP2 is highly dependent on RpoS up regulation since the expression of HP2 is 10-20 times

higher compared to other growth phases, and no difference in the level of expression was detected in *oxyR* knocked-out strain (Schellhorn and Hassan, 1988). The structural gene of HP2, *katE* is mapped at 37.2 min of *E. coli* chromosome. HP2 has a hexameric protein structure consists of 93 kDa subunits (Schellhorn, 1995). Despite the similarity between HP1 and other peroxidase, HP2 shares homology with catalase in other prokaryotes and eukaryotes (Loewen and Triggs, 1984).

2.5.2.1.2 Superoxide dismutase genes

Three types of superoxide dismutase have been identified in *E. coliI*,Mn-superoxide dismutase, Fe-superoxide dismutase, and CuZn-superoxide dismutase (Iuchi and Weiner, 1996). These enzymes are named according to metal groups they contain. They have different roles in the protection against superoxide. Mn and Fe-superoxide dismutase enzymes are present in the cytoplasm (Iuchi and Weiner, 1996; Fee, 1991) while CuZn-superoxide dismutase is located at the periplasmic membrane (Gort et al., 1999). The three enzymes are encoded by *sodA*, *sodB*, and *sodC*, respectively (Fee, 1991; Gort et al., 1999). The absence of these genes can result in high rates of spontaneous mutagenesis, suggesting that the enzymes are crucial in preventing DNA damage (Lynch and Kuramitsu, 2000). Between two cytoplasmic superoxide dismutase, Mg-superoxide dismutase was found to provide highest protection to DNA against oxidative damage, whereas Fe-superoxide dismutase can only provide moderate protection for DNA (Lynch and Kuramitsu, 2000).

sodA encodes a basic dimeric protein consisting of two identical 23 kDa subunits. *sodA* is mapped at 87.5 min of *E. coli* chromosome (Fee, 1991), and its expression is dependent on aerobic condition which activates the expression of this gene (Iuchi and

Weiner, 1996; Lynch and Kuramitsu, 2000). It was also shown that superoxide generating substances such as paraquat can induce its expression. Mn-superoxide dismutase is responsible for a large part of the superoxide dismutase activity in *E. coli* cells, and provides protection to DNA from oxidative damage due to its high affinity to DNA (Iuchi and Weiner, 1996). The expression of *sodA* is also up regulated by RpoS during stationary growth phase. In addition of RpoS, SoxRS can positively regulate the expression of *sodA* (Demple, 1996) while ArcAB (aerobic respiratory control) and Fur (ferric uptake regulation) negatively regulate *sodA* (Tardat and Touati, 1991). Fur, which is a regulatory protein involving in iron uptake in cells, represses a group of genes including *sodA* when it forms complex with ferrous iron (Niederhoffer et al., 1990), whereas the repression from *arcAB* is removed under aerobic condition (Fee, 1991).

sodB encodes an acidic dimeric protein containing two subunits of 21 kDa protein. Its structural gene locates at 36.5 min of *E. coli* chromosome (Fee, 1991). *sodB* is known to be constitutively expressed in all growth phases of *E. coli* (Fee, 1991; Iuchi and Weiner, 1996). In contrast to *sodA*, *sodB* expression is up regulated when bound by Fur-Fe (II), and therefore can be induced using iron (Niederhoffer et al., 1990). However, *sodB* provides only moderate protection against oxidative stress (Iuchi and Weiner, 1996).

sodC, encoded for Cu,Zn-superoxide dismutase, is responsible for protection against extracellular superoxide since this enzyme is located in periplasmic membrane (Korshunov and Imlay, 2002). The expression of *sodC* can be repressed during the exponential phase (Lynch and Kuramitsu, 2000), and depressed when cell enters stationary phase. This effect was found to be responsible by *rpoS*. Besides, expression of *sodC* can

also be repressed by Fnr protein in anaerobic growth condition since the *fnr* mutant exhibit 20 fold higher expression of *sodC* (Gort and Imlay, 1998).

2.5.2.2 Regulatory genes

2.5.2.2.1 *rpoS*

rpoS was first identified as *nur* in an ultraviolet and hydrogen peroxide hypersensitive mutant. Later on, it became known as *katF* or *rpoS*, due to its capability to regulate catalase. *rpoS* encodes a 38 kDa protein with a length of 342 amino acids. This protein serves as an alternative sigma factor (sigma-38), which is necessary for binding between RNA polymerase (RNAP) and *rpoS* regulated gene promoter. Structural gene of *rpoS* is located in an *nlpD-rpoS* dicistronic operon. There are three promoters responsible for the expression of *rpoS*. Two, which are sigma-70 (a vegetative sigma factor) dependent, and govern the expression of *nlpD*, located at an upstream region of *nlpD*. Another promoter is found in an *nlpD* structural gene, and is known to exhibit high activities during a stationary phase suggesting a role as a major promoter for *rpoS* (Eisenstark et al., 1996). High expression of *rpoS* was observed in a stationary phase or under stress conditions such as oxidative and acid stress, and high osmolarity (Talukder et al., 1996). Therefore, it is believed that *rpoS* prepares the cells for dormant state in which nutrient starvation and/or high stress conditions are expected.

It is known that at least 400 genes are related to or governed by *rpoS*, and more genes are expected to be identified (Dong et al., 2008). These *rpoS* regulated genes have various functions including, but not limited to ROS metabolism, DNA protection and repair, cell membrane permeability and transport, amino acid biosynthesis and global gene

regulation. Although *rpoS* is highly expressed in stationary phase, a low level of *rpoS* expression with a high RpoS turnover rate was observed in exponentially growing cells (Schweder et al., 1996; Hengge, 2009). This low level of expression of *rpoS* is initiated by the *nlpD* promoters (Eisenstark et al., 1996). Recent research suggested that *rpoS* also has an important regulatory role during exponential phase of bacterial growth. It was found that not all genes that are regulated by *rpoS* in stationary phase are regulated by *rpoS* in exponential phase. In fact, some of the *rpoS* regulated genes are regulated by *rpoS* in either exponential or stationary phase (Dong et al., 2008). *rpoS* expression can be regulated at transcription and post-transcription (Eisenstark et al., 1996; Demple, 1991). In stationary phase, *rpoS* transcription increases more than three folds compared to exponential phase, and protein stability is increased more than 10 folds (Hengge, 2009).

2.5.2.2.2 *oxyR*

After exposed to a low concentration of hydrogen peroxide, *E. coli* exhibits resistance toward higher doses of hydrogen peroxide (Christman et al., 1985). This corresponds to the activation of OxyR protein, which is a transcription factor. OxyR is a 34 kDa protein containing a disulfide bond at cys-199 and cys-208. Under an aerobic condition, this bond is maintained as thiol; however, under challenging of hydrogen peroxide, this thiol bond is oxidized to disulfide bond (Pomposiello and Demple, 2001). Transcription of *oxyR* dependent genes occurs when OxyR is in an oxidized form. *oxyR* gene is mainly expressed in exponentially growing cells under aerobic condition (Michan et al., 1999). In vivo, this activation of OxyR by hydrogen peroxide can occur in about 30 seconds after exposed to hydrogen peroxide, and the oxidized form of OxyR is maintained

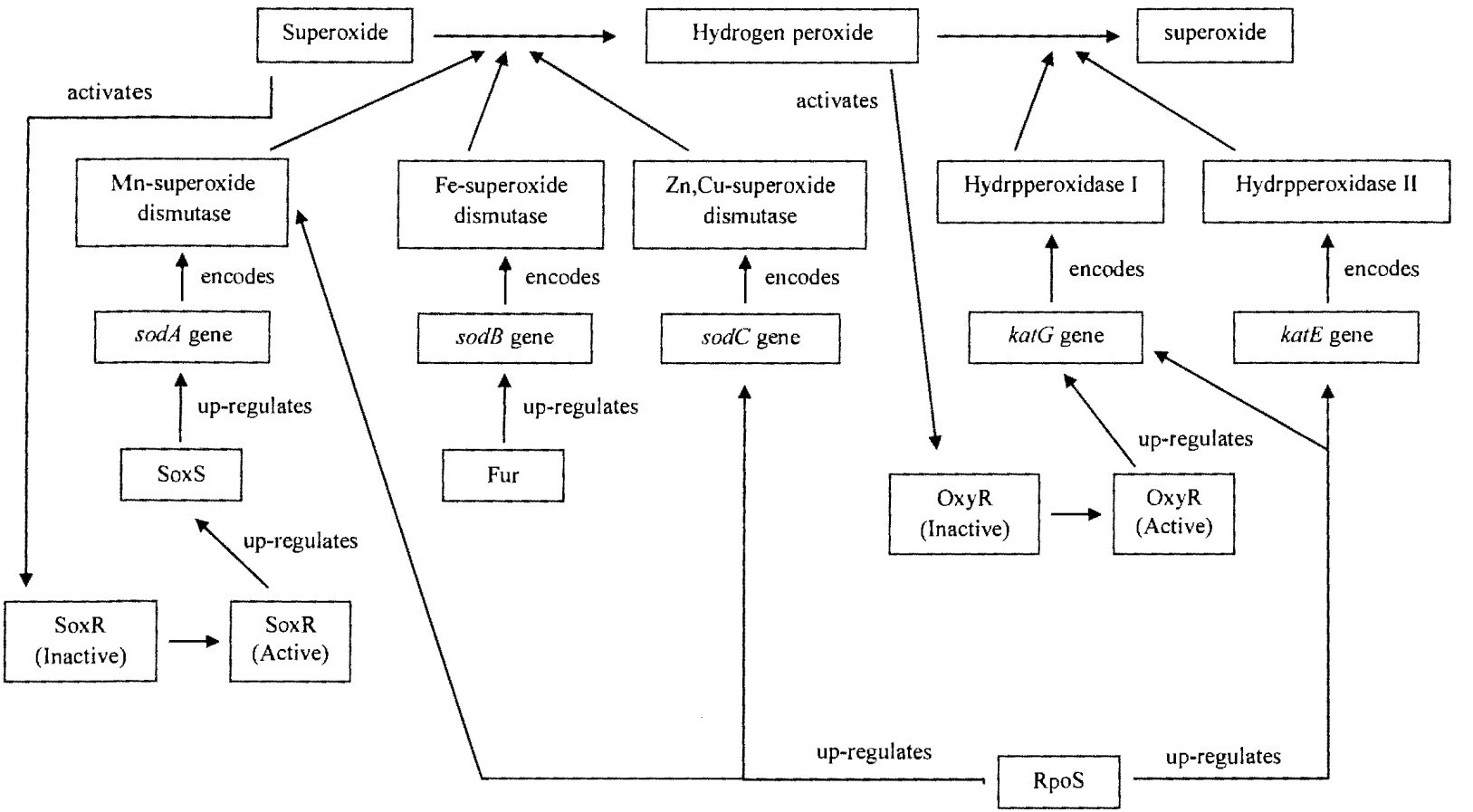

Figure 2.3: A simplified regulatory system of superoxide dismutase and catalase genes

until 5 minutes after the removal of hydrogen peroxide (Pomposiello and Demple, 2001). OxyR can stimulate the synthesis of a small non-coding mRNA namely *oxyS*. This mRNA molecule can affect mRNA stability and translation of at least 20 genes. This function of *oxyS*, allows *oxyR* to indirectly regulate these additional genes (Kim et al., 2002).

2.5.2.2.3 *soxRS*

It has been shown that exposing *E. coli* to a sublethal dose of superoxide producing or inducing agent can trigger oxidative responses which correspond to the regulation of *soxRS*. Both *soxR* and *soxS* encode for transcription activators that are responsible for the expression of at least 16 genes (Greenberg and Demple, 1989; Demple, 1996). These genes have various functions including superoxide transformation by superoxide dismutase and DNA damage repair by endonuclease IV (Demple, 1996). SoxR protein is a dimer of two 27 kDa proteins. It contains a helix-turn-helix motif which is capable of binding with a regulatory region of *soxS*.

SoxR protein is constitutively expressed at a low level. SoxR protein can up regulate the expression of *soxS* gene, and maintains level of SoxS protein at about 50-100 molecules per cell. High affinity of SoxR protein to *soxS* gene regulatory region even when *soxS* is not expressed suggests that SoxR protein binds to the promoter of *soxS* gene by default. The reduced form of SoxR protein, which is inactive, can be activated by oxidizing its [2Fe-2S] cluster on each monomer to [3Fe-3S]. This activation causes a conformational change of SoxR which increases the expression of *soxS* by 100 folds (Pomposiello and Demple, 2001). The element located between -10 and -35 of *soxS* promoter serves as the

binding site for SoxR (Hidalgo and Demple, 1994). The 19 bp spacer between this region and *soxS* transcription initiation site, which is different from 17±1 bp of most spacer in *E. coli*, significantly contributes to the regulation of this regulon since the activation of *soxS* involves remodeling of *soxS* promoter in order to facilitate the expression (Hidalgo and Demple, 1997; Pomposiello and Demple, 2001).

The activation of SoxR, which consequently activates *soxS* expression, is triggered by superoxide stress. In the absence of superoxide stress, SoxR and RNAP bind to *soxS* promoter without activating the expression whereas, with the stress from superoxide, SoxR is oxidized which triggers a conformation change of the SoxR-DNA-RNAP complex and allows transcription of *soxS* to occur. It has been shown that under aerobic growth condition, 95% of *soxR* was in a reduced form (Gaudu and Weiss, 1996) which rapidly disappeared when oxidative stress was introduced. The reduced form of iron sulfur cluster was detected again after oxidative stress was removed. SoxS protein encoded from *soxR* gene is capable of inducing other regulated genes including *sodA* (Pomposiello and Demple, 2001).

2.5.2.2.4 *fur*

fur (ferric uptake regulation) gene was first indentified in a mutant lacking capability to regulate many iron related functions such as synthesis of siderophore (a iron chelating molecule), and membrane proteins necessary for iron uptake (Escolar et al., 1999). fur encodes for a Fur protein with the size of 17 kDa. This dimeric protein once associated with ferrous iron can bind to iron consensus sequences (Escolar et al., 1998; Niederhoffer et al., 1990) within the promoter region of Fur dependent genes, and suppress

the gene transcription down stream of that promoter. The majority of the Fur regulated genes involve the iron scavenging and iron homeostasis but Fur also regulates other genes, which are not directly related to iron homeostasis such as genes related to flagella assembly, chemotaxis, and heat shock responses (Escolar et al., 1999). These genes also include oxidative related gene namely *sodA* and *sodB*. Although Fur is normally a negative regulatory protein controlling Fur dependent genes including *sodA*, it plays a positive regulatory role in *sodB* expression. When a sufficient amount of iron is available in the cells, Fur binds with iron forming a Fur-Fe^{2+} complex, which represses the expression of *sodA*, and activates *sodB* expression (Escolar et al., 1999; Niederhoffer et al., 1990; Tardat and Touati, 1991).

2.5.2.2.5 *arcAB*

Niederhoffer et al. (1990) showed that solely knocking out *fur* gene was not sufficient to completely abrogate the repression of *sodA*, suggesting that *sodA* is not only repressed by Fur. A two components system namely *arc* (aerobic respiratory control) *AB* was discovered contributing to the repression of *sodA* when oxygen is not used as an electron acceptor or under anaerobic condition (Tardat and Touati, 1991). *arcAB* system consists of *arcA* gene, which encodes for a transcriptional regulator, and *arcB* gene, which encodes for a redox sensing molecule (Loui et al., 2009). More than 100 operons are regulated by *arcAB* including genes related to the tricarboxylic acid cycle and energy metabolism (Alexeeva et al., 2000). Under anaerobic condition, ArcB protein, a translational product of *arcB* gene, undergoes phosporylation at His292. Then, the phosphate group is transferred to Asp576 and His717 of ArcB respectively. Subsequently, Asp54 of AcrA, a regulator encoded by *arcA* gene, is phosphorylated by AcrB. The

phosphorylated AcrA becomes active and capable of binding to *arcAB* regulated genes including *sodA*, which in turn represses *sodA* expression.

CHAPTER 3. EFFECTS OF NANOSCALE ZERO-VALENT IRON PARTICLES ON BACTERIAL SURVIVABILITY: ROLE OF GROWTH PHASES

3.1. Introduction

Nanoscale zero valent iron (nZVI) particles are frequently used for environmental remediation due to their capability to transform various toxic contaminants such as halogenated compound and organo-pesticide (Grieger et al., 2010; Liu et al., 2005; Theron et al., 2008). These particles are a nanoscopic counterpart of microscopic zero-valent iron particles which have been used since 1994 in permeable membrane barriers for groundwater remediation of chlorinated compounds (Li et al., 2006; Grieger et al., 2010). nZVI exhibits significantly higher reactivity compared to their microscopic counterpart due to their much smaller size (<100 nm) and in turn more available surface in both laboratory and field demonstrations (Wang and Zhang, 1997; Li et al., 2006; Zhang, 2003). However, environmental remediation by nZVI leads to inevitable release of these particles to the environment and may affect beneficial microorganisms such as element recyclers and contaminant degraders. Therefore, the assessment on the toxicity of nZVI is necessary.

The toxicity of nZVI particles has been investigated. Results showed the potential adverse effects of these particles on living cells including human bronchial epithelial cells (Auffan et al., 2008; Lee et al., 2008; Keenan et al., 2009; Diao and Yao, 2009). The bactericidal effect of these particles was explored and their high toxicity on both Gram negative and positive bacteria was observed. More than 99% inactivation of bacterial cells was reported (Auffan et al., 2008; Lee et al., 2008; Diao and Yao, 2009). Despite the known toxicity of these particles, only limited information on their inactivation mechanism is available. A smaller toxic effect was observed in Gram positive bacteria and no

significant adverse effect was detected in fungi (*Aspergillus versilolar*) (Diao and Yao, 2009) suggesting that membrane and cell wall compositions may affect the toxic effects of these particles. Higher inactivation rates were observed in anaerobic or semi-anaerobic conditions compared to aerobic condition (Lee et al., 2008). Several inactivation mechanisms were proposed including oxidative stress induction, membrane disruption, cell structure damage, and cell function interference (Auffan et al., 2008; Lee et al., 2008; Keenan et al., 2009; Diao and Yao, 2009).

Most, if not all of the previous research examined the toxicity of nZVI and other nanomaterials using bacterial cells cultured from stationary phase. However, the growth of bacteria consists of four major phases; lag, exponential, stationary, and declining phase. Among these phases, the physiological characteristics of bacterial cells are significantly different, and may result in different responses when challenged by toxic substances. Furthermore, the growth of bacteria is affected by environmental factors and nutrient availability. More than one phase of bacterial cells exist in the environment, and studying the toxicity of nZVI on only one phase is not sufficient. In this study, the toxic effect of nZVI on bacterial cells cultured from different growth phases was determined. Furthermore, in order to determine whether physical contact between nZVI and bacterial cells is necessary for the inactivation to occur, the survivability when bacterial cells were exposed to filtrate of nZVI suspension was also investigated.

3.2. Materials and Methods

3.2.1 Nanoscale zero-valent iron particles

nZVI was purchased from Toda Co. Japan as reactive nanoscale iron particles (RNIP). The obtained nZVI was synthesized by reduction of iron oxides using hydrogen gas under high temperature. These particles have a zero-valent iron core and maghemite shell structure. The average diameter of the particles varied between 40 and 70 nm with a specific area of 23 to 29 m^2/g (Phenrat et al., 2006; Liu et al., 2005; Nurmi et al., 2004). nZVI, which was originally in a paste form, was dried and kept under nitrogen gas saturated condition in order to limit the oxidation of particles.

3.2.2 Bacterial strains

Four bacterial strains were used in this study including *E. coli* JM109 and *E. coli* BW25113 from Coli Genetic Stock Center at Yale University, *Pseudomonas putida* KT2440 (ATCC47054), and *Pseudomonas putida* F1 (ATCC700007). *E. coli* strains were selected for this study due to their role as a model organism. *P. putida* strains which are normally found in environment were chosen for representing indigenous microbes. Prior to use, each permanent stock culture was grown on nutrient agar in order to determine the purity. Then, a single colony was grown in appropriate media overnight. Growth characteristics of the four bacterial strains were determined by adding 1% v/v of the overnight bacterial culture to 100 mL fresh medium. Then, the number of bacterial cells at different time intervals was determined by a plate count method. In this study, both *E. coli* strains were cultured in tryptic soy broth (TSB) at 37°C, and *P. putida* strains were cultured

in brain heart infusion broth (BHI) at 30°C. Orbital shaking at 150 rpm (Innovo®40) was applied during the cultivation to provide aeration.

3.2.3 Bacterial inactivation by nZVI

3.2.3.1 Bacterial inactivation by 1 g/L of nZVI

Bacterial cells were collected at predetermined time points based on the growth characteristic of each strain (Table 3.1). One percent (v/v) of the overnight culture was added to 100 ml of fresh medium. At each time point, bacterial cells were collected by centrifugation at 6,000 g for 5 minutes. The collected cells were washed twice using 150 mM PBS buffer (pH 7.2), and resuspended in 2 mM carbonate buffer (pH 8.0). The final cell concentration was adjusted to 1×10^6 to 3×10^6 CFU/ml in 25 ml of the same carbonate buffer followed by the addition of nZVI to a concentration of 1000 mg/L. This relatively high concentration was selected since the practical field concentration of nZVI is between 2 to 10 g/L, which is subsequently diluted once injected into groundwater. Mixing of the bacteria with nZVI was provided by vigorous stirring using a magnetic stirrer (Coring PC-353 Stirrer) at 1500 rpm, and viable cells were determined at 0, 5, 10, 15, 30, and 60 minutes by a plate count method. In order to assure that cells from the correct growth phase were obtained, bacterial growth was also monitored during the cultivation by a plate count method. All of the experiments were triplicated. In each replicate, all the cells from different time points were collected from the same batch of the culture.

3.2.3.2 Inactivation of bacterial cells by different concentrations of nZVI

In the case of JM109, the nZVI concentrations of 90, 200, 500, and 800 mg/L were also experimented in order to examine the responses of these cells to lower doses of nZVI.

As described previously, bacterial cells were harvested at the appropriated time points (Table 3.1). The collected cells were mix with 90, 200, 500, or 800 mg/L of nZVI. Viable cells were determined at 0, 5, 10, 15, 30, and 60 minutes after cells were exposed to nZVI by a plate count method. All of the experiments were triplicated. In each replicate, samples were collected from the same batch of bacterial culture.

Table 3.1: Selected time points for bacterial cultivation

Strain	**Time (hour)**											
	Lag	**Exponential**			**Stationary**						**Decline**	
***E. coli* JM109**	1	2.5	4	5.5	-	12	16	24	48	72	84	96
***E. coli* BW25113**	0.5	2	3.5	5	-	12	16	24	48	72	84	96
***P. putida* KT2440**	0.5	-	2	3.5	8	12	16	24	48	72	96	120
***P. putida* F1**	0.5	-	2	3.5	8	12	16	24	48	72	96	120

3.2.3.3 Inactivation using nZVI suspension filtrate

The filtrate of nZVI suspension was prepared by adding 1000 mg/L of nZVI in 2 mM carbonate buffer (pH 8.0) followed by 1 hour of vigorous stirring with a magnetic stirrer (Coring PC-353 Stirrer) at 1500 rpm. The suspension was filtered through a 0.20 μm pore size membrane filter to remove particles. Only JM109 cells were used in this experiment. The cells were collected and washed as previously described. Finally the cells were resuspended in 25 mL of the filtrate to the concentration of 1×10^6 to3×10^6 CFU/ml. Cell viability was determined by a plate count method. The experiment was triplicated, and in each replicate, all the cells from different time points were collected from the same batch of culture.

3.2.4 Statistical analysis and LD_{50} determination

All the results of cell inactivation were analyzed using the Statistical Analysis System (SAS ver. 4.2) software. In each bacterial strain, data of all the time points from each growth phase (Table 1) were combined to represent each individual phase results. Analysis was conducted by least significant difference *t*-test with 95% confidence. Fifty percent lethal dose (LD_{50}) for each growth phase of JM109 was determined. Effect of different doses of nZVI at 10 minutes after contact to bacterial cells was combined together. Subsequently, the concentration which inactivates 50% of bacterial cells was calculated.

3.3. Results and Discussion

3.3.1 Effect of nZVI on bacterial cells from different growth phases

The cell survival of *E. coli* JM109 and BW25113 following exposure to nZVI in different growth phases is shown in Figures 3.1 and 3.2. Among the different growth phases of JM109, early and mid-exponential (2.5 and 4 hour cultivation) and declining phases (84 and 96 hour cultivation) exhibited the lowest resistance to nZVI with 3.5, 2.8, 2.8 and 4 log inactivation for cells harvested at 2.5, 4, 84, and 96 hours respectively after 1 hour exposure to nZVI. However, cells in late exponential (5.5 hour cultivation) showed a lower inactivation rate, which is similar to cells in stationary phase. These results suggest that cells at late exponential phase might have higher resistance to nZVI. Comparing to exponential and declining phases, cells in lag and stationary phases exhibited higher resistance (1.7 log inactivation observed for lag phase cells and less than 2.4 log inactivation for all time points in stationary phase cells).

Similarly, higher resistance to nZVI was found in cells from lag and stationary phases of BW25113, and lower resistance in exponential and declining phases was also observed. The high resistance of bacteria in stationary phase might result from cell adaptation to stressful environments (Ishihama, 1997) since the phase normally has limited nutrient and necessary substrate for bacterial growth. Furthermore, one of the proposed toxic effects of nZVI is oxidative stress induction (Auffan et al., 2008; Lee et al., 2008) which normally occurs in stationary phase (Lushchak, 2001). Hence, cells in stationary phase exhibit many defensive mechanisms to mitigate the adverse effects resulting from oxidative stress, such as defensive enzymes (i.e. superoxide dismutase, catalase, and dehydratase), protective protein (dnp), and damage repairing enzymes (i.e. endunuclease and exonuclease) (Lushchak, 2001; Storz, Tartaglia, Farr et al., 1990; Touati, 2000). Although, high resistance to nZVI was observed in both lag and stationary phase cells, statistic analysis suggests that only cells cultured from stationary phase exhibited significantly higher resistance to nZVI.

The overall inactivation rate by nZVI in BW25113 was higher than JM109. All the results for BW25113, except early log (1.1 log inactivation) and declining phases (1.4 log inactivation), showed less than 1 log inactivation at 30 minutes inactivation whereas, for JM109, exposure to nZVI for 30 minutes resulted in greater than 1 log inactivation. Moreover, BW25113 also exhibited higher resistance to nZVI than JM109 since the highest inactivation found in BW25113 was 2.7 log inactivation, whereas 4 log inactivation was observed in JM109 cells Bacterial inactivation of *P. putida* KT2440 is shown in Figure 3.3. For strain KT2440, the observed cell inactivation and inactivation rate were much lower than in *E. coli* strains. No greater than 1 log inactivation was detected in KT2440. The

resistance to nZVI was even higher in F1 in which only limited inactivation (less than 0.4 log inactivation) was detected (Figure 3.4). The overall resistance to nZVI of four bacterial strains ranged from high to low in the following order: *P. putida* F1, *P. putida* KT2440, *E. coli* BW25113, and *E. coli* JM109. These results suggest that the toxic effects of nZVI on bacterial cells are not only species dependent, but also strain dependent. The summary of different bacterial strains inactivation was shown in Table 3.2. For the results in exponential, stationary, and declining phases, which had more than one samples, inactivation results from all the samples obtained from the same phase were averaged.

Table 3.2: Bacterial cell survival after inactivation by 1000 mg/L of nZVI for 1 hour

Strain	**Log inactivation of bacterial cells**			
	Lag	**Exponential**	**Stationary**	**Decline**
***E. coli* JM109**	1.68	2.65	2.02	3.36
***E. coli* BW25113**	0.75	1.32	0.90	2.22
***P. putida* KT2440**	0.74	0.78	0.54	0.56
***P. putida* F1**	0.32	0.32	0.26	0.26

3.3.2 Inactivation of bacterial cells by different concentrations of nZVI

The inactivation of JM109 was further investigated using lower concentrations of nZVI since this strain exhibited lowest resistance to nZVI among the four strains. Results indicated that the level of cell inactivation corresponded to the concentration of nZVI. Higher concentration such as 1000, 800, and 500 mg/L of nZVI (Figures 3.1, 3.5, and 3.6) exhibited rapid and high bacterial cell inactivation whereas 200 and 90 mg/L of nZVI (Figures 3.7 and 3.8) only had limited effects on cell viability. Nonetheless, bacterial cell inactivation was observed in all concentrations used in this experiment. By using these data, the LD_{50} of nZVI to JM109 cells in each growth phase was also determined.

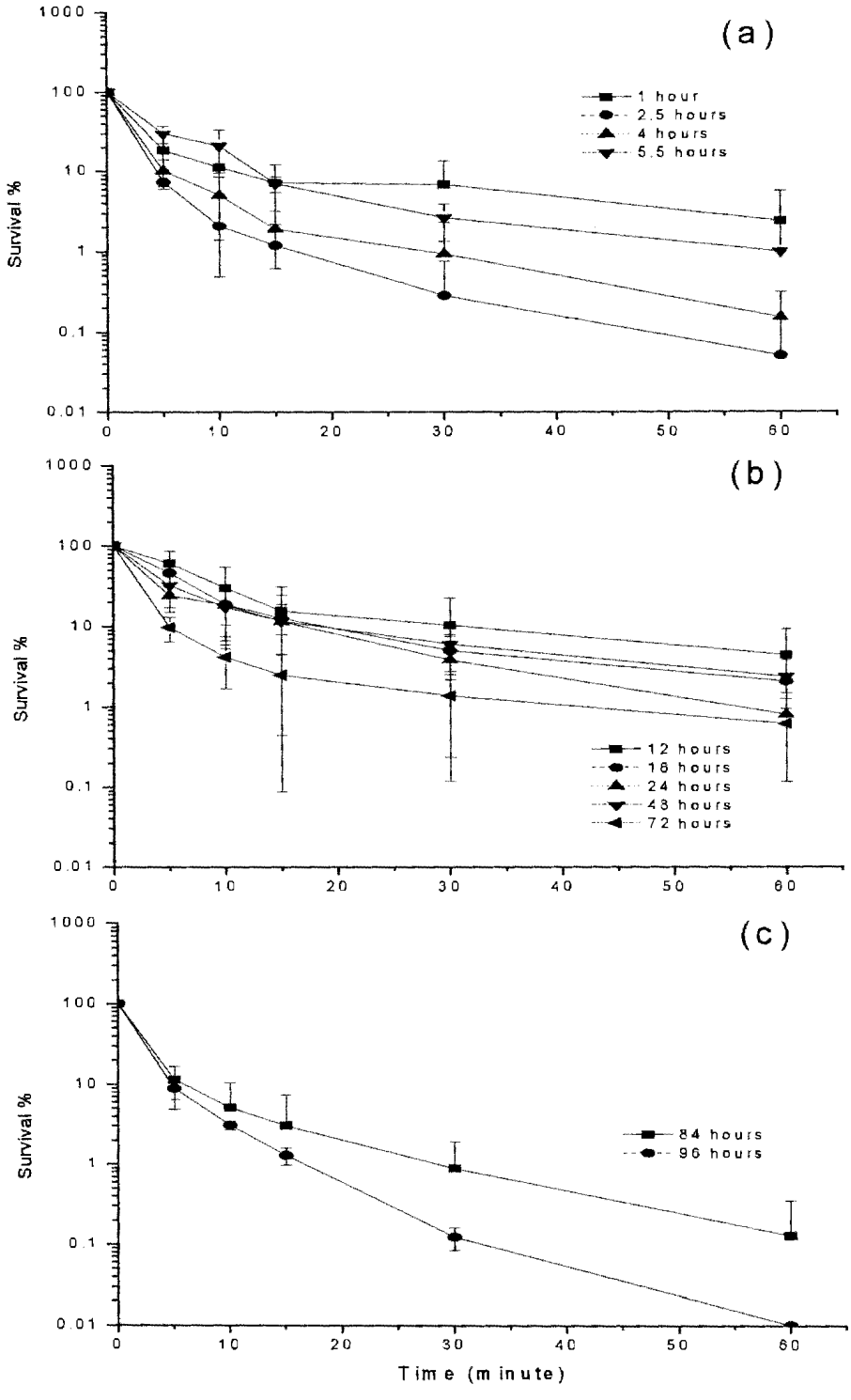

Figure 3.1: Inactivation of *E. coli* JM109 cultured from (a) lag and exponential phases, (b) stationary phase, and (c) declining phase using 1000 mg/L of nZVI

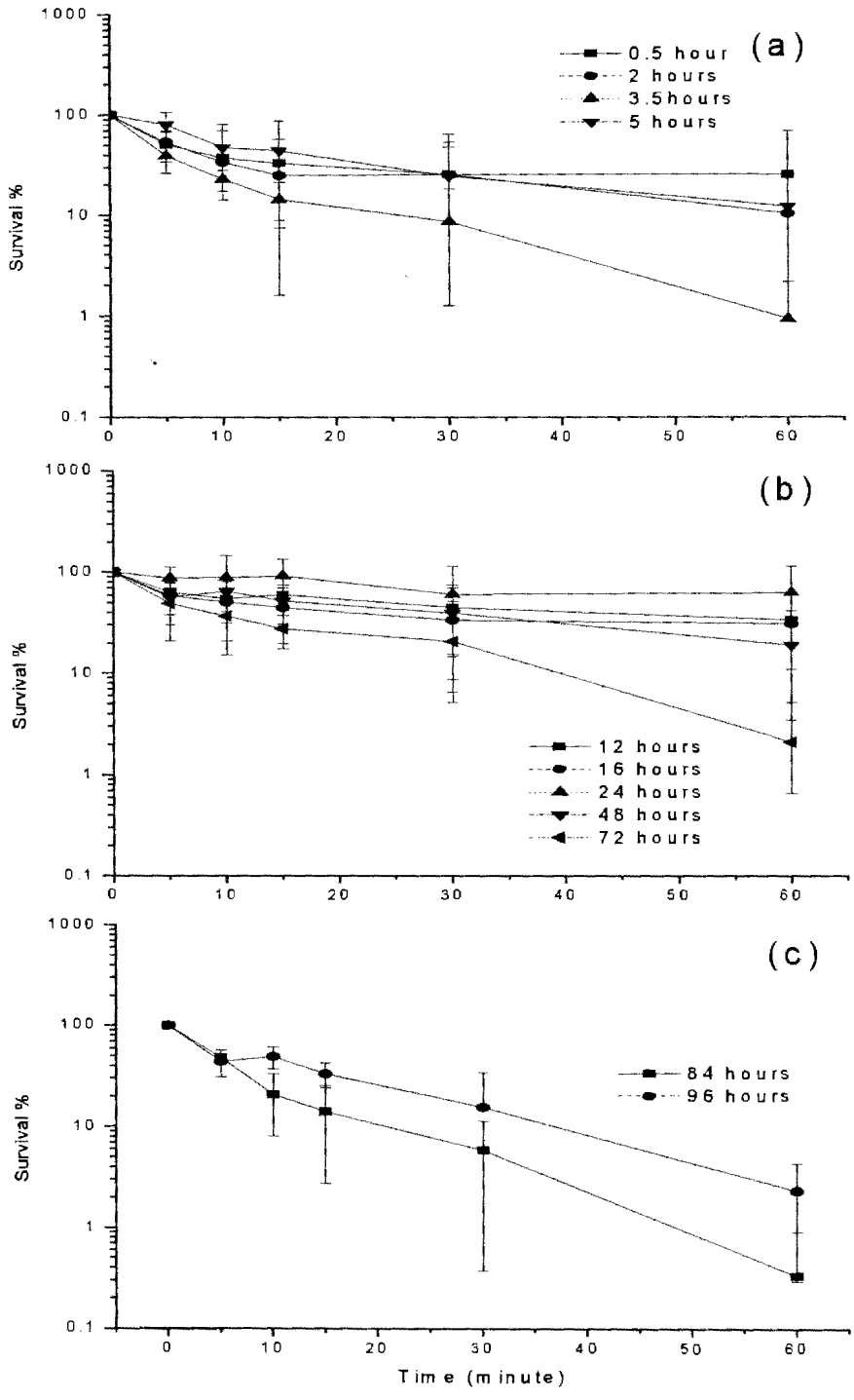

Figure 3.2: Inactivation of *E. coli* BW25113 cultured from (a) lag and exponential phases, (b) stationary phase, and (c) declining phase using 1000 mg/L of nZVI

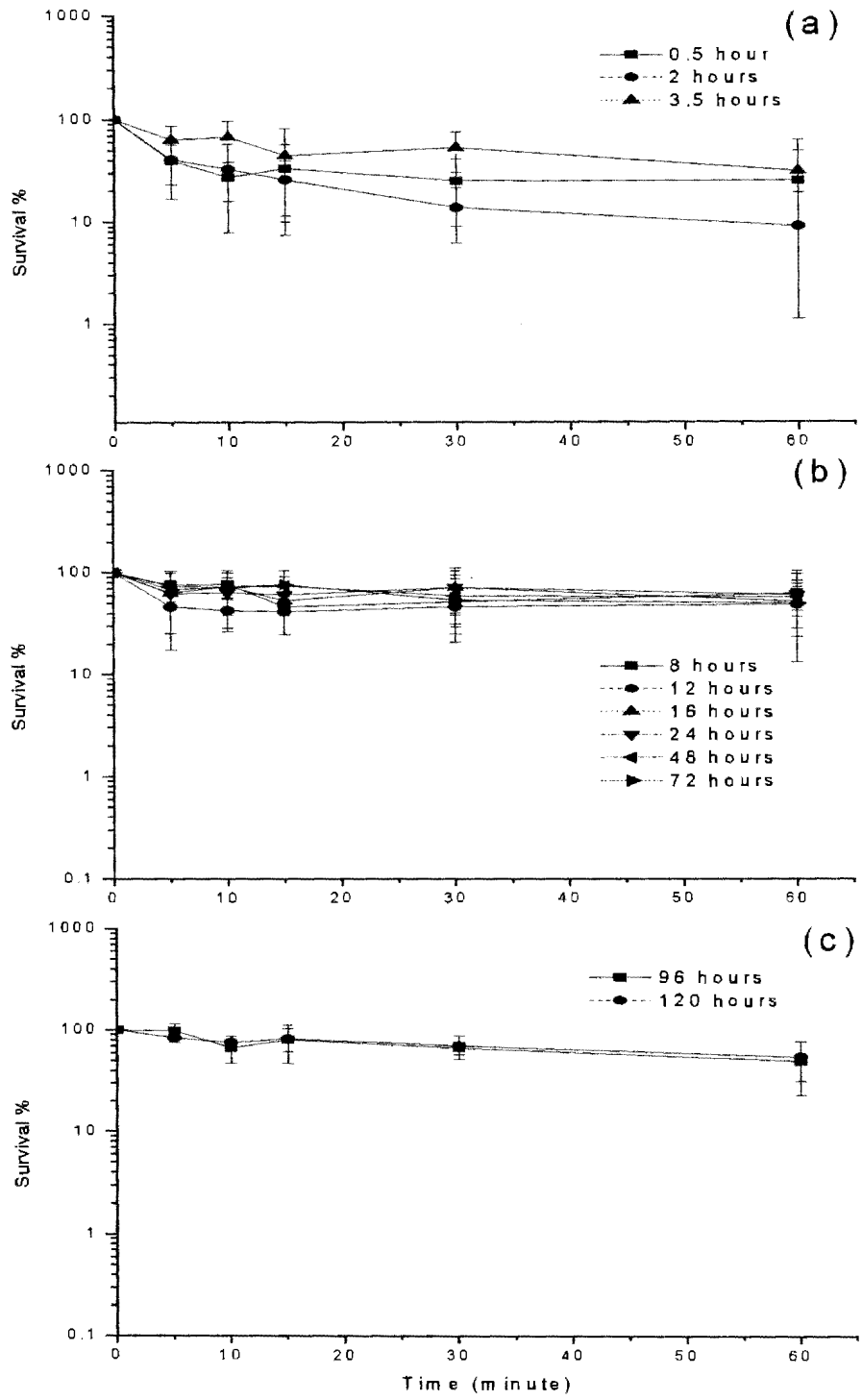

Figure 3.3: Inactivation of *P. putida* KT2440 cultured from (a) lag and exponential phases, (b) stationary phase, and (c) declining phase using 1000 mg/L of nZVI

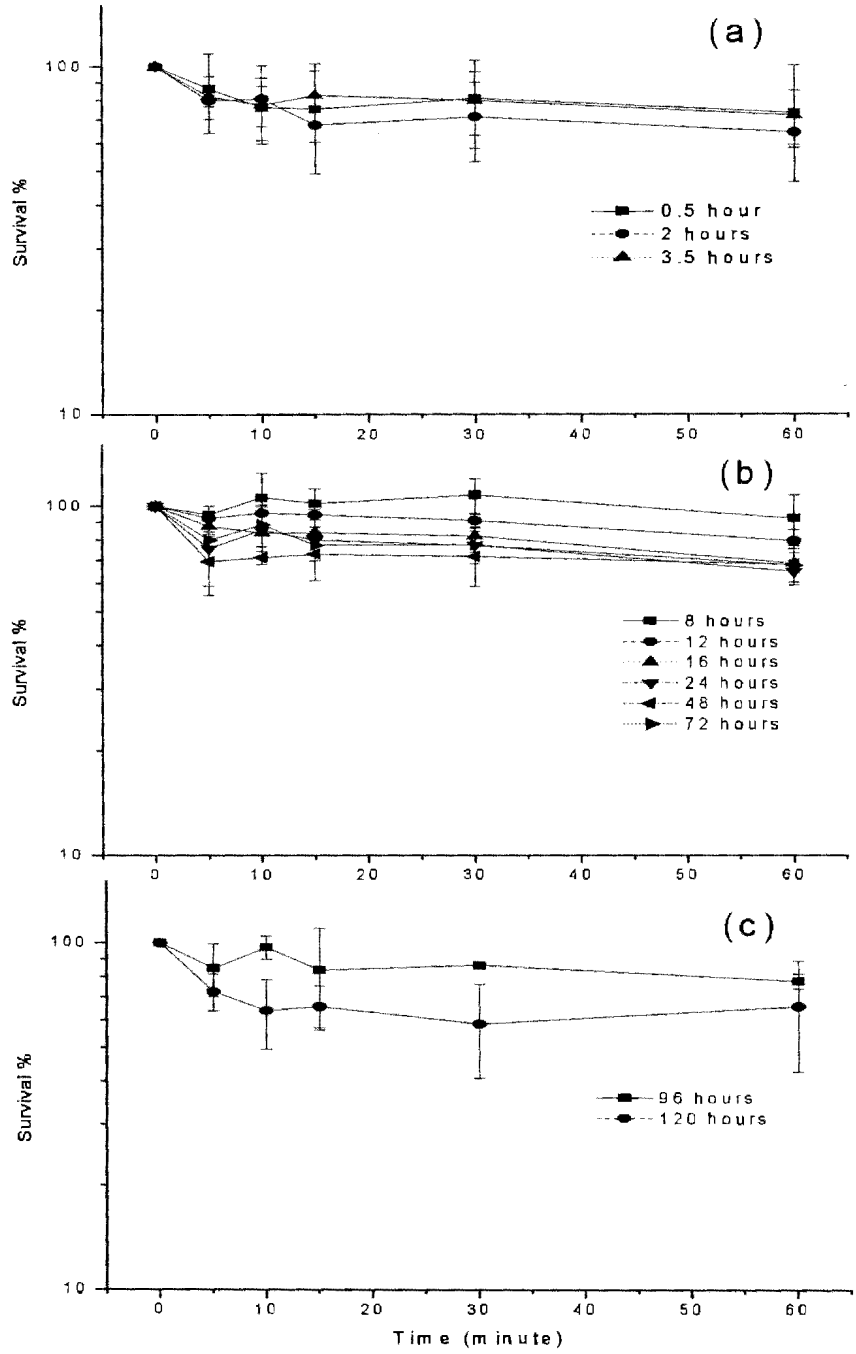

Figure 3.4: Inactivation of *P. putida* F1 cultured from (a) lag and exponential phases, (b) stationary phase, and (c) declining phase using 1000 mg/L of nZVI

At 10 minute inactivation time, the the LD_{50} for cell in lag, exponential, stationary, and decline phases were 427, 380, 527, and 329 mg/L respectively. Since the resistance to nZVI of cells in stationary phase was relatively high, LD50 of stationary phase cells was also higher compared to LD50 of other phases. The inactivation of JM109 cells by different concentrations of nZVI was summarized in Table 3.3.

Table 3.3: Cell inactivation by different concentrations of nZVI for 1 hour

nZVI concentration	**Log inactivation of bacterial cells (JM109)**			
	Lag	**Exponential**	**Stationary**	**Decline**
1000 mg/L	1.68	2.32	2.02	3.36
800 mg/L	2.87	2.65	2.51	3.26
500 mg/L	1.23	1.51	1.54	2.17
200 mg/L	1.12	1.17	0.86	1.02
90 mg/L	0.71	0.75	0.92	1.35

3.3.3 Effect of nZVI suspension filtrate on bacterial survivability

Inactivation using nZVI suspension filtrate was investigated in JM109 in order to determine the significance of physical interaction between bacterial cells and nZVI for cell inactivation. JM109 was selected because this strain showed the least resistance to nZVI. Very minimal cell inactivation (14% cell inactivation) (Figure 3.9) was detected when JM109 was exposed to the nZVI filtrate. This suggests that the physical presence or interaction between bacterial cells and nZVI is important for bacterial inactivation.

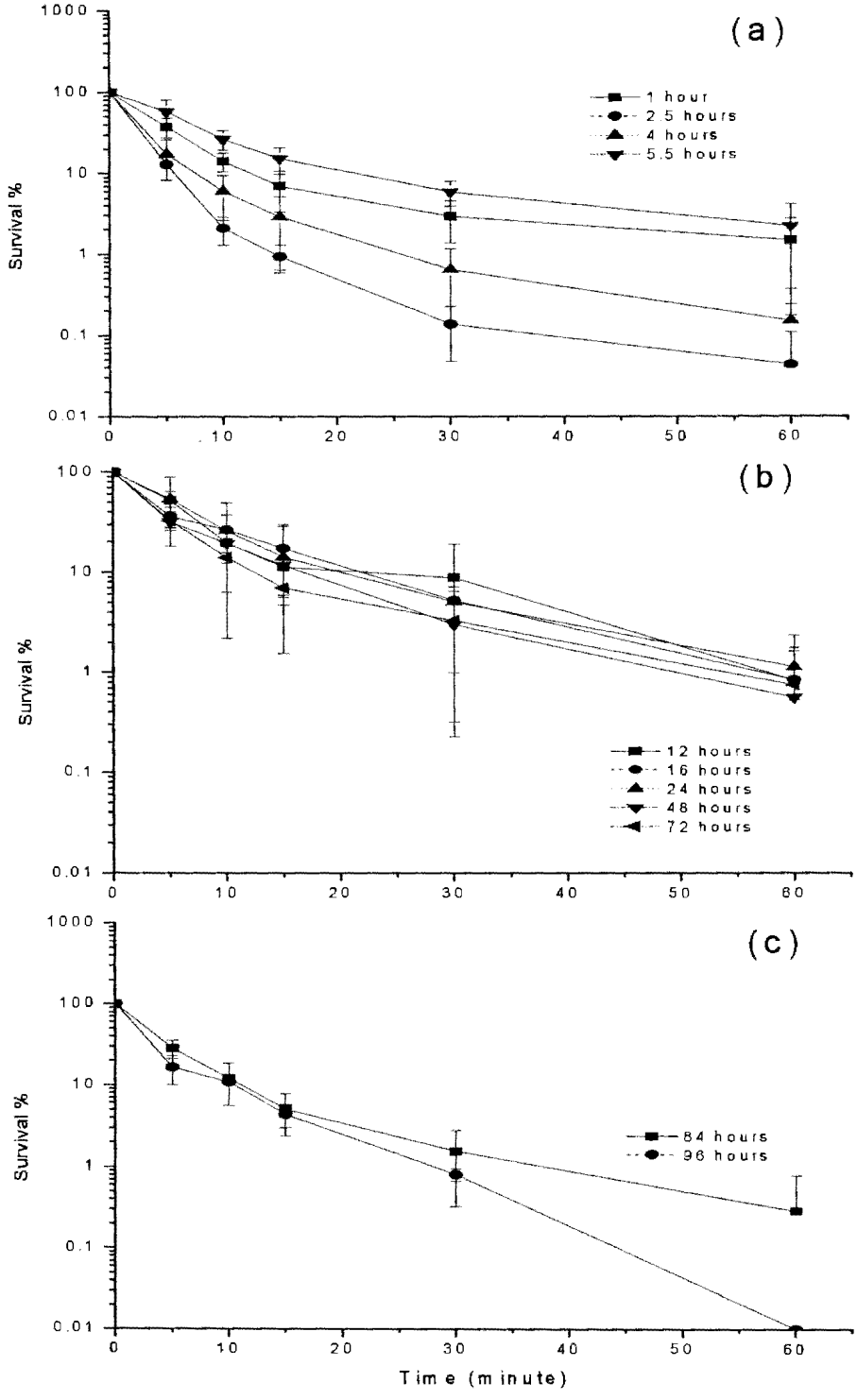

Figure 3.5: Inactivation of *E. coli* JM109 cultured from (a) lag and exponential phases, (b) stationary phase, and (c) declining phase using 800 mg/L of nZVI

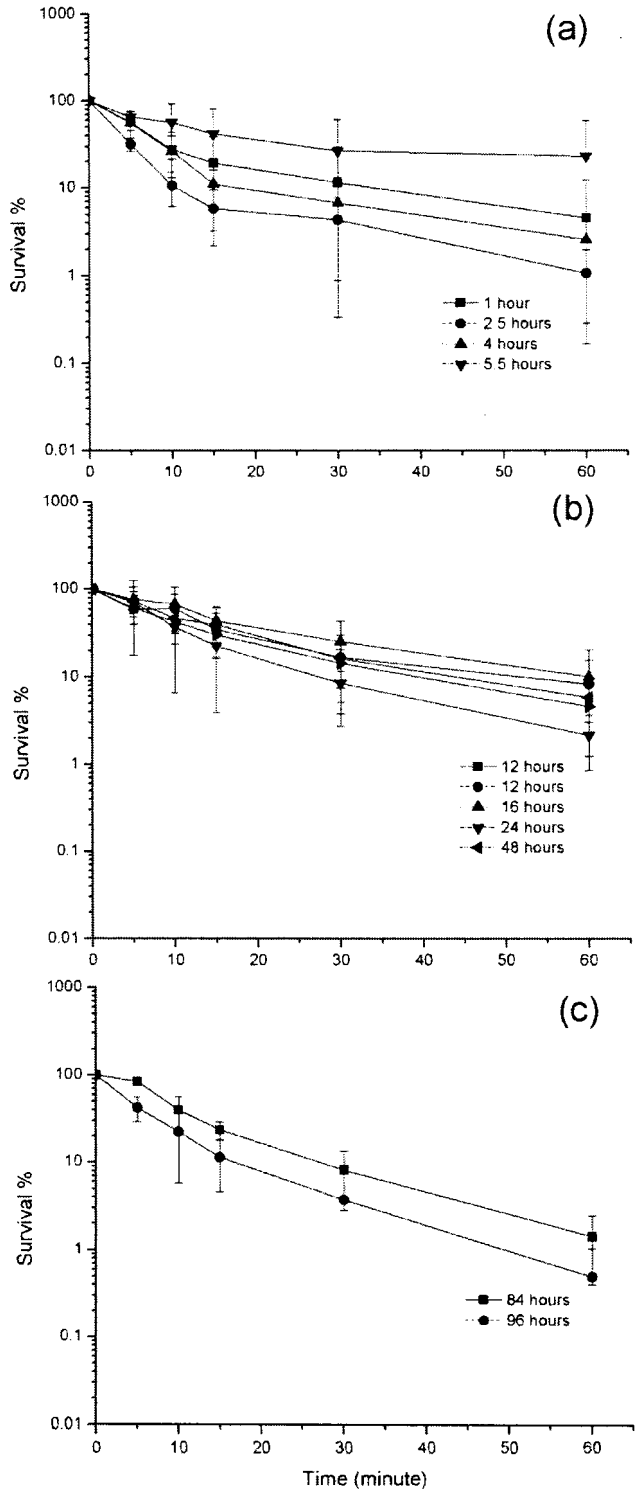

Figure 3.6: Inactivation of *E. coli* JM109 cultured from (a) lag and exponential phases, (b) stationary phase, and (c) declining phase using 500 mg/L of nZVI

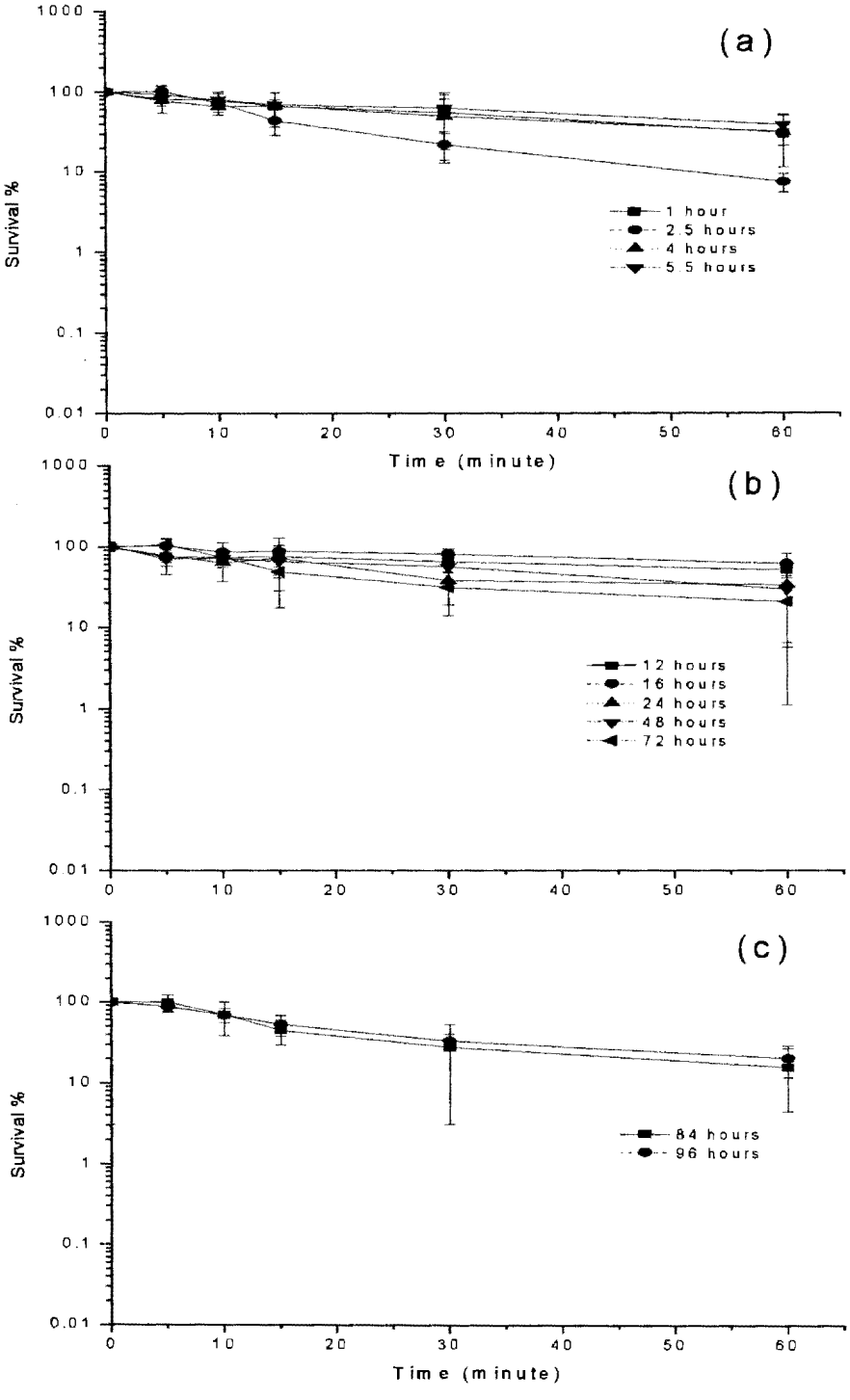

Figure 3.7: Inactivation of *E. coli* JM109 cultured from (a) lag and exponential phases, (b) stationary phase, and (c) declining phase using 200 mg/L of nZVI

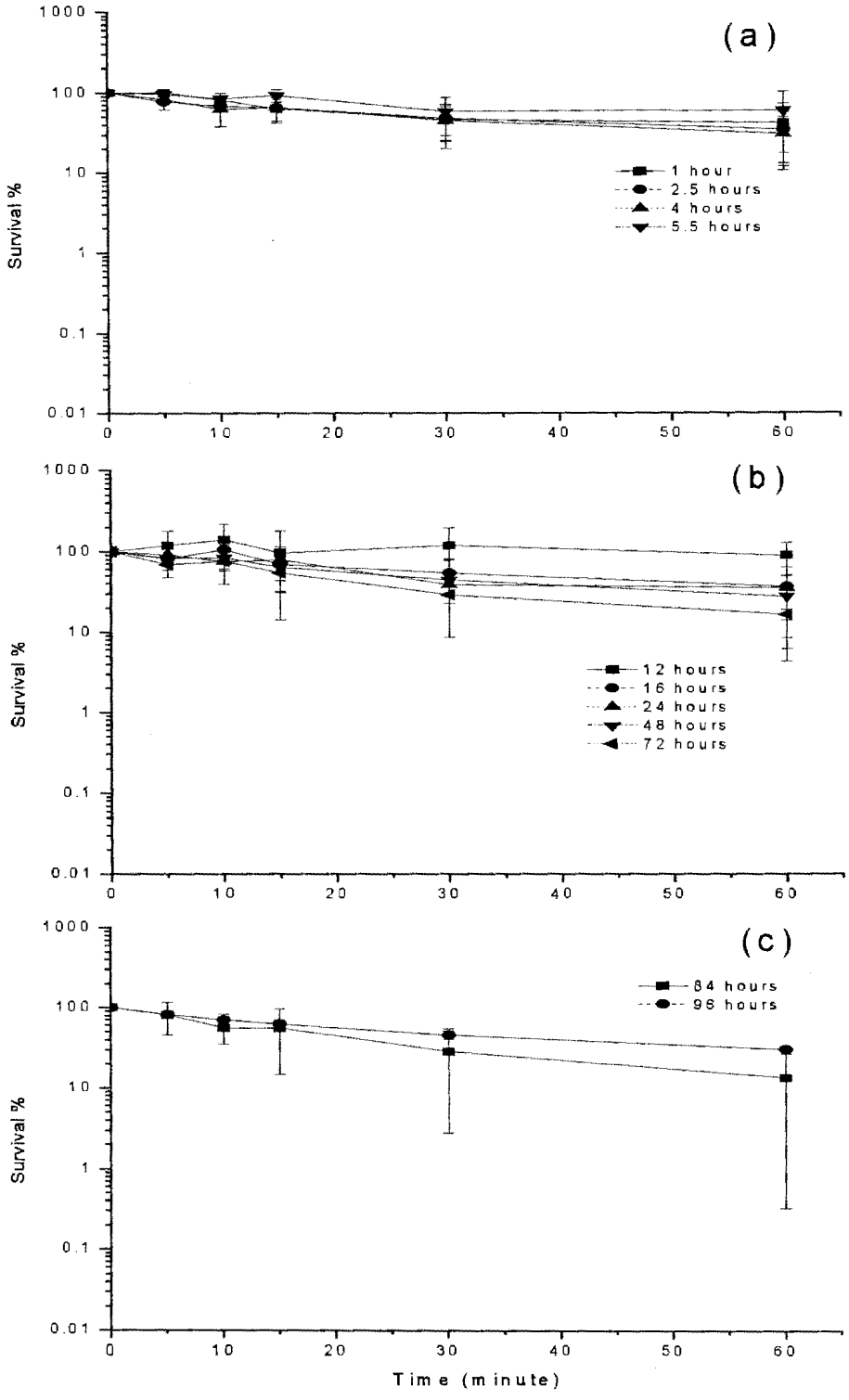

Figure 3.8: Inactivation of *E. coli* JM109 cultured from (a) lag and exponential phases, (b) stationary phase, and (c) declining phase using 90 mg/L of nZVI

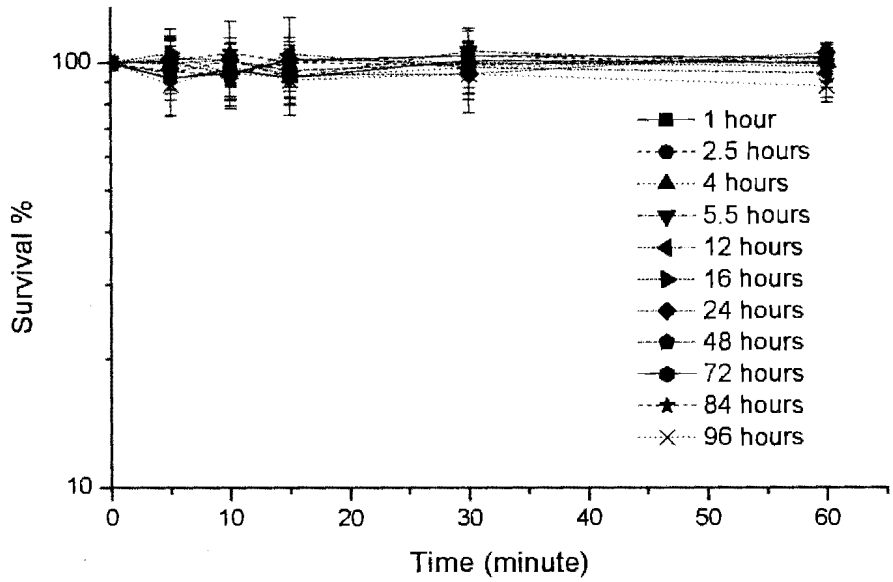

Figure 3.9: Inactivation of *E. coli* JM109 by nZVI suspension filtrate

3.4. Summary

In this chapter, the toxic effect of nZVI on bacterial cells harvested from different growth phases was examined. Higher resistance to nZVI was observed in cells from lag and stationary phases, whereas cells from exponential and declining phases exhibited less resistance to nZVI. The results also suggest that the effect of nZVI on bacteria was both species and strain dependent. The effect of nZVI also depended on the concentration of the particles. The results from exposure of bacterial cells to nZVI suspension filtrate suggest that physical interaction between cells and nZVI is crucial for cell inactivation.

CHAPTER 4. ROLE OF OXIDATIVE STRESS IN BACTERIAL INACTIVATION BY NANOSCALE ZERO-VALENT IRON

4.1. Introduction

The improvement of nanotechnology during the last few decades has greatly increased the applications of nanomaterials and nanoparticles in various fields. Many of these applications were in environmental remediation since various nanomaterials and nanoparticles such as carbon nanotubes, TiO_2, and iron based particles can remediate many toxic contaminants (Grieger et al., 2010; Theron et al., 2008). Among nanoparticles, nZVI is frequently used for degradation, detoxification, or transformation of various halogenated organic compounds, which were normally found in contaminated sites, due to higher reactivity and faster cleanup time compared to some other remediation technologies (Li et al., 2006; Liu et al., 2005; Zhang, 2003; Grieger et al., 2010).

Despite the wide applications of these nZVI, several studies suggested that these particles can cause adverse effects on living cells, which include both prokaryotic and eukaryotic cells. Exposure of high concentrations of nZVI to human bronchial epithelial cells can rapidly inactivate these cells (Keenan et al., 2009). Toxic effects of nZVI toward both Gram negative and Gram positive bacterial cells have also been reported (Lee et al., 2008; Auffan et al., 2008; Diao and Yao, 2009). The toxic effect of nZVI may affect beneficial indigenous microbes in the environment such as contaminant degraders and element recyclers (Barnes et al., 2010) since significant amounts of these particles are directly released to the environment through the environmental remediation processes (Grieger et al., 2010). A recent study revealed that nZVI can potentially be used as a low-cost and high efficiency disinfectant for water (Diao and Yao, 2009).

Although recent studies indicated the toxicity of nZVI, the mechanism in which living cells are inactivated by nZVI mostly remains unclear. In order to understand and mitigate the effects of nZVI on cells and organisms, more insight on the inactivation mechanism is necessary. Several mechanisms were proposed in recent studies including oxidative stress induction, membrane and cell components disruption, and cell function interference (Lee et al., 2008; Auffan et al., 2008; Keenan et al., 2009; Diao and Yao, 2009). Auffan et al. (2008) observed higher susceptibility to nZVI in a mutant lacking oxidative stress related enzymes.

Oxidative stress refers to a stress condition which is induced by several oxygen containing molecules or ROS when these ROS overcome the defensive capability of the cell (Lushchak, 2001). ROS such as superoxide anion, hydrogen peroxide, and hydroxyl radical are constitutively generated in aerobically growing cells. One of these ROS namely superoxide radical is produced when oxygen molecule, which serves as a final electron acceptor in the electron transport chain, accepts an electron (Storz, Tartaglia, Farr et al., 1990; González-Flecha and Demple, 1995).

ROS exhibit high reactivity to all components inside the cells including lipids, proteins, and nucleic acids (Lushchak, 2001; Nel et al., 2006). Therefore, aerobically growing cells require defensive mechanisms against these damages from ROS such as damage prevention, ROS scavenging, and damage repair (Lushchak, 2001; Iuchi and Weiner, 1996; Storz, Tartaglia, Farr et al., 1990; Demple, 1991). These defensive mechanisms are accomplished by a significant number of genes encoding for defensive enzymes, signaling molecules, protective molecules and regulatory proteins which enable tremendous control of these responses toward oxidative stress (Eisenstark et al., 1996;

Lushchak, 2001). Interestingly, hydroxyl radical, which is also one of the main ROS, might not be significantly involved in nZVI toxicity toward bacterial cells since no significant difference in cell viability was observed when adding hydroxyl radical scavenger into the inactivation reaction (Lee et al., 2008).

Catalase and superoxide dismutase enzymes are known to be important to the defensive mechanism against oxidative stress, mainly by changing the high reactivity oxygen containing molecules to less reactive molecules (Schellhorn, 1995; Fee, 1991; Gort et al., 1999). Therefore *katG* and *katE*, which encode for catalase, and *sodA*, *sodB*, and *sodC* which encode for superoxide dismutase were also crucial for bacterial survival in an oxidative stress condition. Typically, superoxide radical from aerobic respiration is converted into hydrogen peroxide which is another ROS. Subsequently, enzymes containing catalase activity transform hydrogen peroxide to oxygen and water.

RpoS, a well-known global regulator for various stress responses to acid stress, starvation, pH, temperature and high osmolarity, also contributes to responses toward oxidative stress (Dong et al., 2008; Eisenstark et al., 1996; Hengge, 2009; Talukder et al., 1996). RpoS is an alternative sigma factor controlling the expression of more than 400 genes which includes *sodC*, *katE*, *katG*, and other genes related to oxidative stress. RpoS is highly expressed in stationary phase whereas relatively low level of expression was found in exponential phase. Nonetheless, a recent study indicated that, even with a low level of expression in exponential phase, it still has a crucial regulatory role over a significant number of genes in exponential growing cells. Several genes are regulated by RpoS in either exponential or stationary phase (Dong et al., 2008).

In order to assess the toxic effect of nZVI, it is necessary to understand the mechanism by which the living cells are inactivated. In a study described in Chapter 3, the responses of bacterial cell in different growth phases to nZVI were determined, and higher resistance in stationary phase cells was observed. Moreover, the expression of many oxidative stress related genes is highly dependent on the growth phase. Thus in this study, the role of oxidative stress as an inactivating mechanism of nZVI was evaluated by examining the survival and susceptibility of several bacterial knocked-out mutants lacking oxidative stress defensive enzymes. The knocked-out genes encode superoxide dismutase, catalase, and a global stress regulatory protein—RpoS. The survivability of these mutants throughout the bacterial cultivation was determined, and compared with their wild-type strain. The inducibility of *katG* by nZVI during the bacterial growth was also investigated by measuring and comparing the expression of *katG* in bacterial cells with and without exposure to nZVI.

4.2. Materials and Methods

4.2.1 Nanoscale zero-valent iron particles

Commercial nZVI was obtained from Toda Co. Japan, as reactive nanoscale iron particles. These nZVI particles were synthesized by reduction of iron oxides using nitrogen gas. The particles had a size range of 40 to 70 nm and a specific area of 23 to 29 m^2/g (Phenrat et al., 2006; Liu et al., 2005; Nurmi et al., 2004). The nZVI in a paste form was dried and kept under nitrogen gas saturated condition to prevent oxidation of these particles.

4.2.2 Bacterial strains

Wild-type *E. coli* BW25113 was used for this study. Six mutants of *E. coli* including JW3879-1 (Δ*sodA*), JW1648-1 (Δ*sodB*), JW1638-1 (Δ*sodC*), JW3914-1(Δ*katG*), JW1721-1 (Δ*katE*), and JW5437-1 (Δ*rpoS*) were obtained from the Coli Genetic Stock Center at Yale University and used in this study. Before use, the purity of the permanent bacterial stock culture was determined on nutrient agar. Subsequently, the culture was reactivated by transferring a single colony to fresh TSB medium and incubated overnight. Bacterial growth characteristic was determined by adding 1% v/v of each overnight bacterial culture to 100 mL of TSB at 37°C and 150 rpm orbital shaking (Innova®40). The bacterial cell numbers were determined by a plate count method at appropriate time points.

4.2.3 Bacterial inactivation by nZVI

Bacterial cells were harvested at predetermined time points as follows: 0.5 hour for lag phase, 2, 3.5, and 5 hours for exponential phase, 12, 16, 24, 48, and 72 hours for stationary phase, and 84 and 96 hours for declining phase. Initially, 1% v/v of the overnight culture was transferred to 100 mL culture medium. Bacterial cells at each predetermined time point were harvested by centrifugation at 6,000 g for 5 minutes. The collected cells were washed twice in 150 mM PBS buffer (pH 7.2), and resuspended in 2 mM carbonate buffer (pH 8.0). The final cell concentration was between 1×10^6 and 3×10^6 CFU/mL in 25 mL of the same carbonate buffer. nZVI was added to the final concentration of 1,000 mg/L. This concentration was selected since, in field applications of nZVI, up to 10 g/L of these particles are injected into the ground water, and subsequently diluted into lower concentrations. Mixing was provided by using a magnetic stirrer (Coring PC-353 Stirrer) at

1500 rpm. The number of viable cells at 0, 5, 10, 15, 30, and 60 minutes after exposed to nZVI was determined by a plate count method on nutrient agar. In order to assure that the desired bacterial growth phases were obtained, bacterial growth was monitored during the cultivation by a plate count method. All experiments were conducted in triplicate, and in each replicate, all the samples in different time points were collected from the same batch of bacterial culture.

4.2.4 Expression of *katG* gene

katG, which encodes for catalase, is inducible by exposure to sublethal concentrations of hydrogen peroxide (Christman et al, 1985). In order to determine whether *katG* is inducible by nZVI, the expression of *katG* in cells before and after being exposed to nZVI was investigated. A 1% (v/v) inoculum of the overnight BW25113 culture was added to TSB medium, and bacterial cells at 0.5, 2, 3.5, 5, 12, 16, 24, and 48 hours of cultivation were collected. At each time point, two samples were collected and total RNA of the first sample without nZVI exposure was stabilized by RNAprotect Bacteria Agent (Qiagen). The second sample was washed twice and then exposed to nZVI. In order to obtain enough cells for RNA extraction after nZVI exposure, 500 mg/L of nZVI was used rather than the higher concentration used in previous experiment (1000 mg/L), and the inactivation time was also reduced to 30 minutes. After exposure to nZVI, cells were collected and total RNA was stabilized. The stabilized RNA was isolated using RNeasy mini prep (Qiagen) according to the instruction provided by the manufacturer. The extracted RNA was treated with RNase-Free-DNase (Qiagen) in order to remove contaminated DNA.

cDNA was synthesized from extracted RNA using a random primer (Promega) and Moloney Murine Leukemia Virus reverse transcriptase (Promega). Reverse transcription was carried out at 37°C for 60 minutes followed by enzyme inactivation by heating at 70°C for 10 minutes. Sample without reverse transcriptase served as a negative control. The concentration of cDNA was determined by quantitative polymerase chain reaction (qPCR) using a PCR system (Real-time, Model 7500, Applied Biosystems) with 16sRNA as a normalizing gene. This normalizing gene was selected due to its constitutive expression of this gene in all the growth phases. All *katG* expressions were normalized, and *katG* expression after inactivation by nZVI was related to *katG* expression before exposure to nZVI. The sequences of 5′-CCT CGC TGG CGG ATA TCA-3′and 5′-GCG GCT TTC TCA ACA CCA A -3′ were used for forward and reverse primers of *katG* gene. 5′-CCA GGG CTA CAC ACG TGT TA-3′and 5′-TCT CGC GAG GTC GCT TCT-3′were used as forward and reverse primers for *16sRNA* gene, respectively. 6FAMAGT GCT GGC TGG TGT GMGBNFQ and VICAAT GGC GCA TAC AAAMGBNFQ served as probes for *katG* and *16sRNA* respectively. All the primers were designed using Primer Express® Software (Applied Biosystems). A qPCR reaction using molecular grade water instead of cDNA was used as a negative control. The experiment was triplicated and each replicate was duplicated in qPCR.

4.2.5 Statistical analysis

All the results from the cell inactivation experiment were analyzed using the Statistical Analysis System (SAS ver. 4.2) software. Data at 2, 3.5, and 5 hours time points were combined to represent the exponential phase results. Similarly, data for all time points

were combined for the stationary and declining phases. Analysis was conducted by least significant difference *t*-test with 95% confidence.

4.3 Results and Discussion

4.3.1 Inactivation of oxidative stress related mutants

Survivability of a wildtype strain (BW25113) and its six oxidative stress related mutant strains lacking of superoxide dismutase (*sodA*, *sodB*, and *sodC*), catalase (*katG* and *katE*), and sigma-s-factor (*rpoS*) are shown in Figures 4.1 to 4.4. Among cells in lag phase, *rpoS*, *sodA*, and *sodB* mutants showed higher susceptibility to nZVI compared to BW25113 strain (Figure 4.1). Cell survivability among these three mutants was relatively similar for the first 15 minutes of nZVI exposure but after 15 minutes of inactivation, the *rpoS* mutant exhibited higher susceptibility to nZVI than the *sodA* and *sodB* mutants. About 1.5 and 1.7 log inactivation in *sodA* and *sodB* mutants and more than 2 log inactivation in *rpoS* mutant were observed after 1 hour inactivation by nZVI.

In the exponential phase (Figure 4.2), relatively high inactivation was observed in several mutants including those lacking of *rpoS* and superoxide dismutase. About 4 log inactivation was detected in *rpoS*, *sodA*, *sodB*, and *sodC* mutants during early exponential phase (2 hour cultivation) (Figure 4.2a). High inactivation rate was also observable during mid-exponential phase (Figure 4.2b), especially for *sodA* and *sodB* mutants, which exhibited more than 4 log inactivation after 1 hour exposure to nZVI. This suggests that superoxide dismutase, especially Mg- and Fe-superoxide dismutase play an important role in cell protection against nZVI when cells are actively growing. Moreover, the high susceptibility of *rpoS* mutant in exponential phase suggests that, although *rpoS* is highly

expressed only in stationary phase (Talukder et al., 1996), *rpoS* might also be responsible for the oxidative stress responses in exponential phase. This is supported by a study of Dong et al. (2008) which indicated that *rpoS* also has a significant regulatory role in actively growing cells.

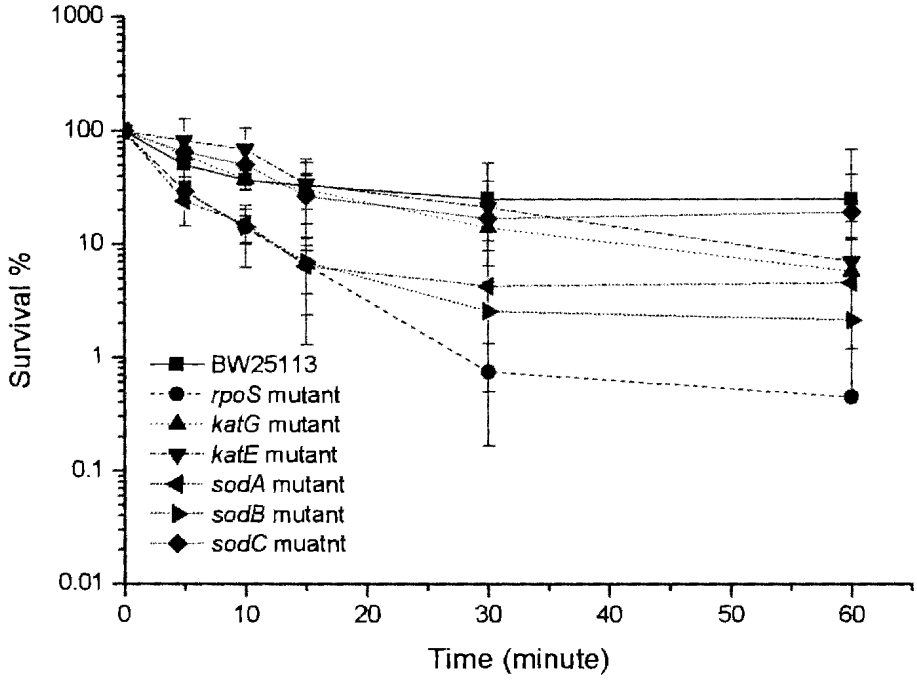

Figure 4.1: Inactivation of bacterial cells in lag phase (0.5 hours cultivation) by 1000 mg/L of nZVI

Interestingly, the inactivation rate in late exponential phase of most of the mutants was lower than their mid-log inactivation rate (Figure 4.2c). This might due to the adaptation of bacterial cells toward stationary phase since cells in stationary phase exhibited higher resistance to nZVI (as described in Chapter 3). This was further confirmed by the inactivation of cells from stationary phase, in which all the mutants except *rpoS* showed less than 2 log inactivation after exposure to nZVI for 1 hour (Figure 4.3 and 4.4).

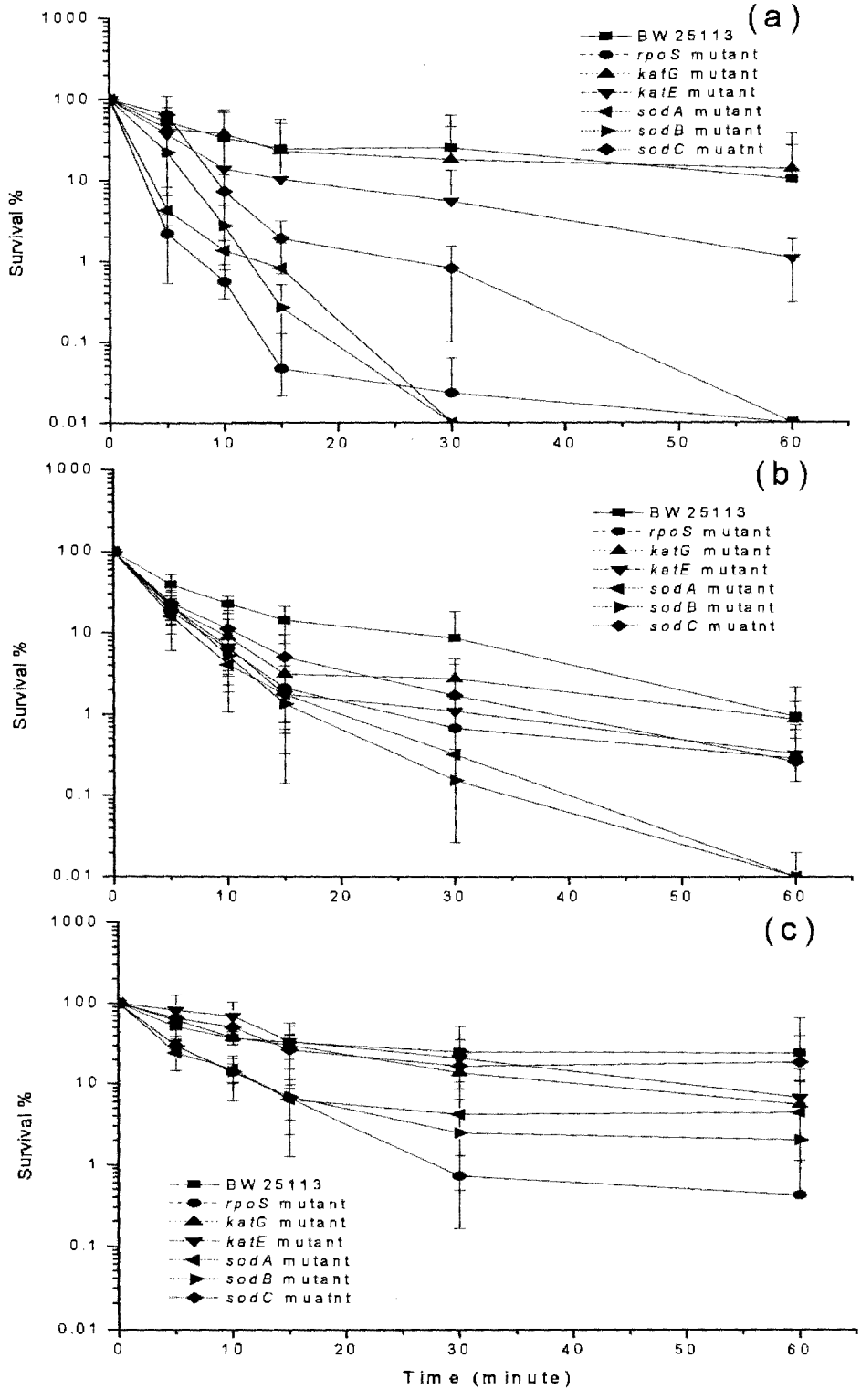

Figure 4.2: Inactivation of bacterial cells in exponential phase harvested at (a) 2 hours cultivation, (b) 3.5 hours cultivation, and (c) 5 hours cultivation by 1000 mg/L of nZVI

For the *rpoS* mutant, more than 2 log inactivation was observed from samples taken at 12 to 72 hour cultivation times (Figures 4.3, and 4.4). Samples from longer cultivation time also exhibited more rapid inactivation. The *rpoS* mutant at 24 hours cultivation showed 1.2 log inactivation after exposing to nZVI for 10 minutes whereas, in cells from 48 hours cultivation, 2 log inactivation was observed at 10 minutes after inactivation by nZVI.

The susceptibility of cells lacking of *rpoS* in stationary phase suggests that RpoS, as a sigma factor, has a vital role in cell protection against nZVI. Moreover, since *katE* and *sodB* expressions in stationary phase are directly regulated by *rpoS* (Tanaka et al., 1997; Fee, 1991; Eisenstark et al., 1996), the high susceptibility of the *rpoS* mutant, which was much higher than the inactivation of *katE* and *sodB* mutants, suggest that other genes regulated by *rpoS* might also have an important role in cell protection against nZVI. All the cells from declining phase exhibited more than 1 log inactivation when exposed to nZVI (Figure 4.5). However, when compared to the wildtype strain, only *rpoS*, *sodA*, *sodB*, and *katE* mutants showed relatively higher susceptibility. Only limited relative susceptibility was observed in *sodC* mutant.

The statistical analysis of data is shown in Table 4.1. Among cells cultured from lag and exponential phases, *sodA*, *sodB*, and *rpoS* mutants exhibited significantly higher susceptibility toward nZVI. No significant difference in cell survival was detected in *katG*, *katE*, and *sodC* mutants. In stationary phase cells, significantly higher susceptibility was observed only in *rpoS* mutant. *sodA*, *sodB*, and *rpoS* mutants, *katE* mutant also showed higher susceptibility in declining phase. Although no significant level of susceptibility to nZVI was detected in *katG*, and *sodC* mutants from all four phases, and *katE* mutant in lag,

exponential, and stationary phases respectively, it is noteworthy that most of these mutants exhibit higher inactivation rates when exposed to nZVI compared to the wildtype strain.

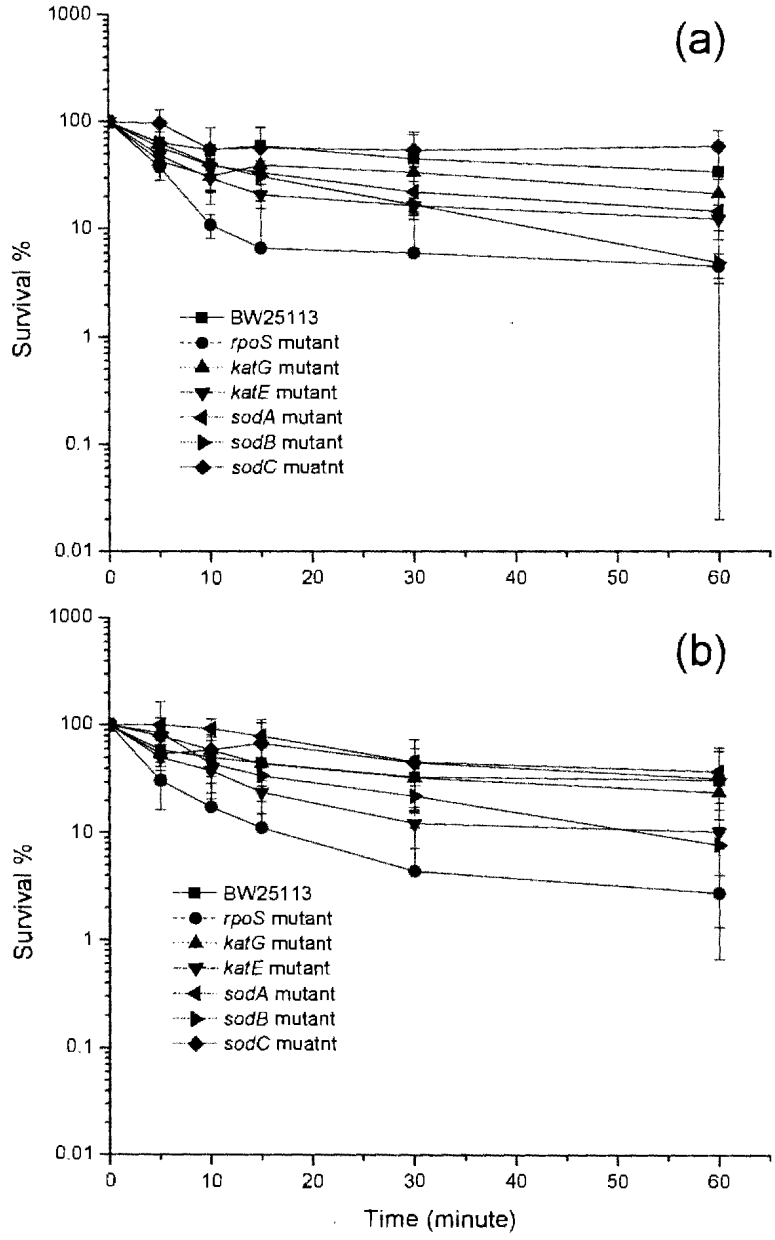

Figure 4.3: Inactivation of bacterial cells in exponential phase harvested at (a) 12 hours cultivation, and (b) 16 hours cultivation by 1000 mg/L of nZVI

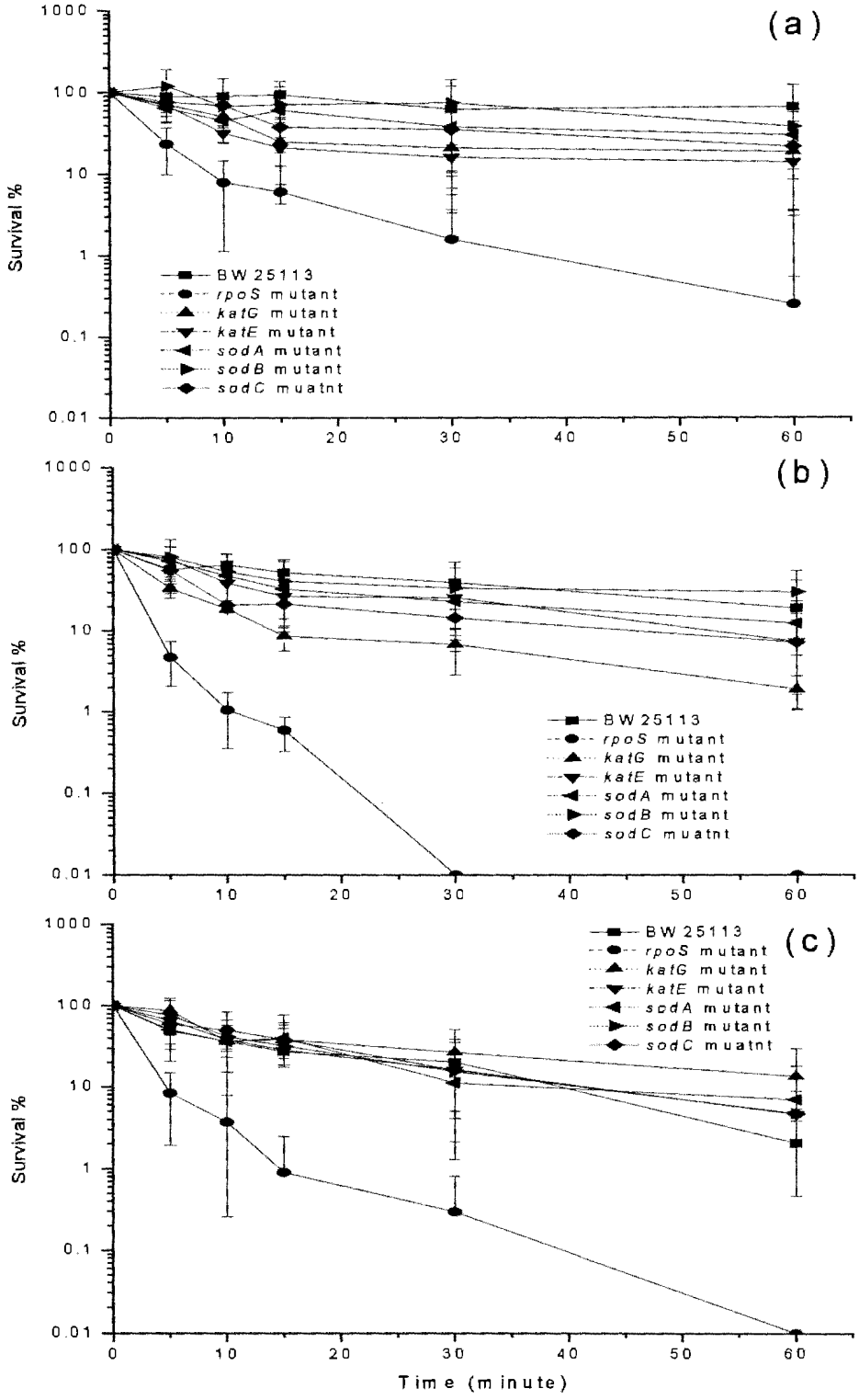

Figure 4.4: Inactivation of bacterial cells in stationary phase harvested at (a) 24 hours cultivation, (b) 48 hours cultivation, and (c) 72 hours cultivation by 1000 mg/L of nZVI

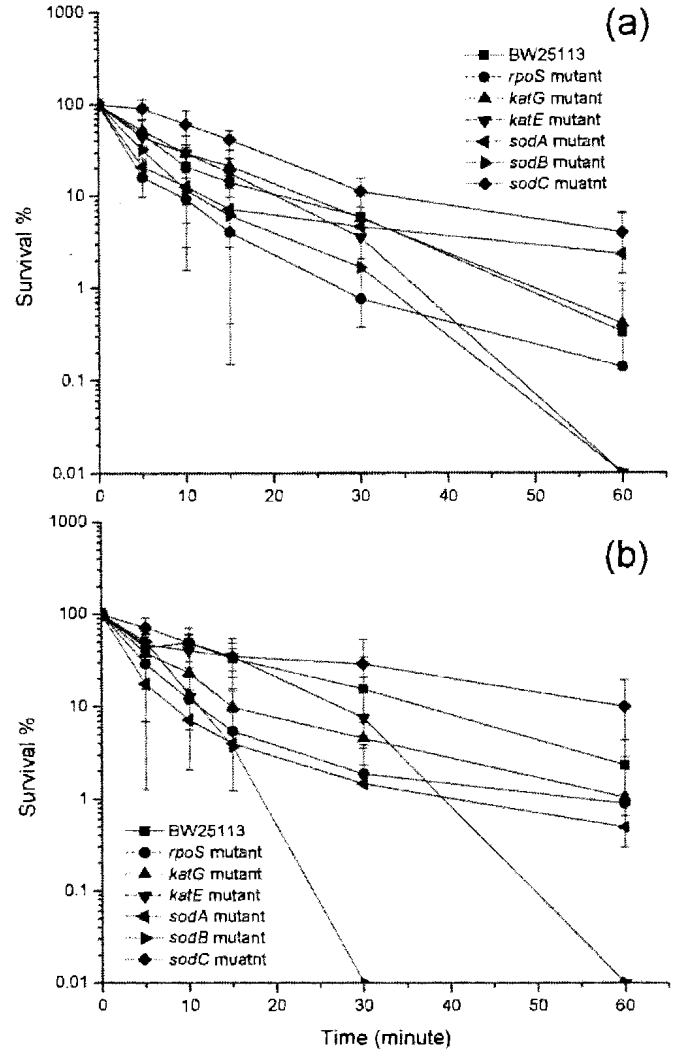

Figure 4.5: Inactivation of bacterial cells in declining phase harvested at (a) 84 hours cultivation and (b) 96 hours cultivation by 1000 mg/L of nZVI

Overall, the observed toxic effects. were higher in strains lacking superoxide dismutase genes (*sodA* and *sodB*) compared to strains lacking catalase genes suggesting that superoxide dismutase might be more critical than catalase in protecting cells against ROS generated from nZVI. On the contrary, according to the survivability of the *katG* and *katE* mutants, hydrogen peroxide might not significantly contribute to cell inactivation. Lee et al. (2008) indicated that hydroxyl radical did not significantly contribute to the toxic

Table 4.1: Statistical analysis results of oxidative stress related mutant inactivation

Growth Phase	Mutant					
	rpoS	*sodA*	*sodB*	*sodC*	*katG*	*katE*
Lag	+	+	+	-	-	-
Exponential	+	+	+	-	-	-
Stationary	+	-	-	-	-	-
Decline	+	+	+	-	-	+

"+" indicates significant difference in survivability from wildtype strain
"-" indicates no significant deference in survivability from wildtype strain

effect of nZVI. Therefore superoxide radical might be the main ROS generated from nZVI when oxygen is present. However, among three types of superoxide dismutase namely Mg-superoxide dismutase, Fe-superoxide dismutase, and Cu/Zn-superoxide dismutase which are encoded by *sodA*, *sodB*, and *sodC* genes respectively, only stains without *sodA* and *sodB* which encode for cytolosic superoxide dismutase (Lynch and Kuramitsu, 2000), but not *sodC* gene which encodes for periplasmic superoxide dismutase (Korshunov and Imlay, 2002) showed higher susceptibility to nZVI. Therefore, our results suggest that the oxidative stress induced by nZVI might result from induction and/or generation of superoxide inside the cell. A conceptual model illustrating a possible inactivation mechanism by nZVI was shown in Figure 4.6. When cells are exposed to nZVI particles, these particles either bind to or penetrate through cell membrane, and induce oxidative stress by generating superoxide inside cells.

4.3.2 Inducibility of *katG* by nZVI

Inducibility of *katG*, which is the expression of *katG* after exposure to nZVI relative to *katG* expression without inactivation, is shown in Figure 4.7. At lag phase, the expression of *katG* after exposure to nZVI was about two folds higher than the expression

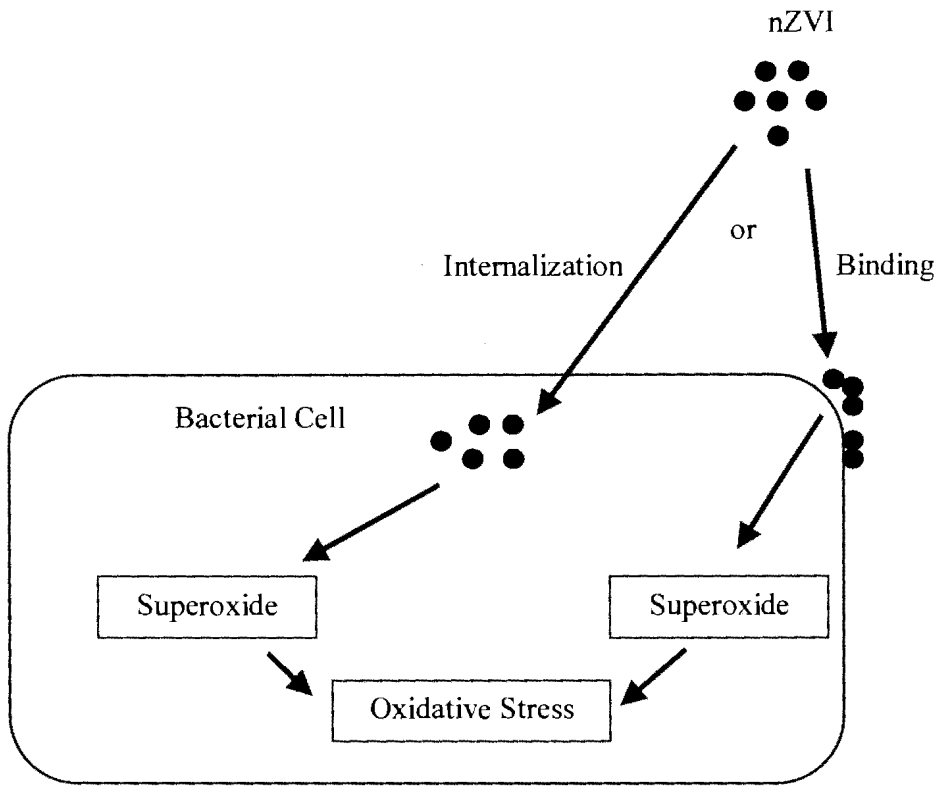

Figure 4.6: A conceptual model of cell inactivation by nZVI

without exposure. This indicates that *katG* in lag phase is inducible by nZVI. However, the inducibility of *katG* by nZVI was not observed after cells entered exponential phase. On the contrary, repression of *katG* expression was observed. At early exponential phase, *katG* expression was about the same level as without nZVI exposure. When cells reached mid-exponential phase, repression of *katG* was observed after exposure to nZVI. Furthermore, *katG* expression remained repressed in cells cultured from other growth phases. Similarly, the repression of gene expression was also observed in a study conducted by Xiu et al. (2010) in which two genes namely *tceA* and *vcrA* encoding for reductive dehalogenase were down regulated after exposed to nZVI. These results suggest that nZVI might correlate with the suppression of certain gene expressions.

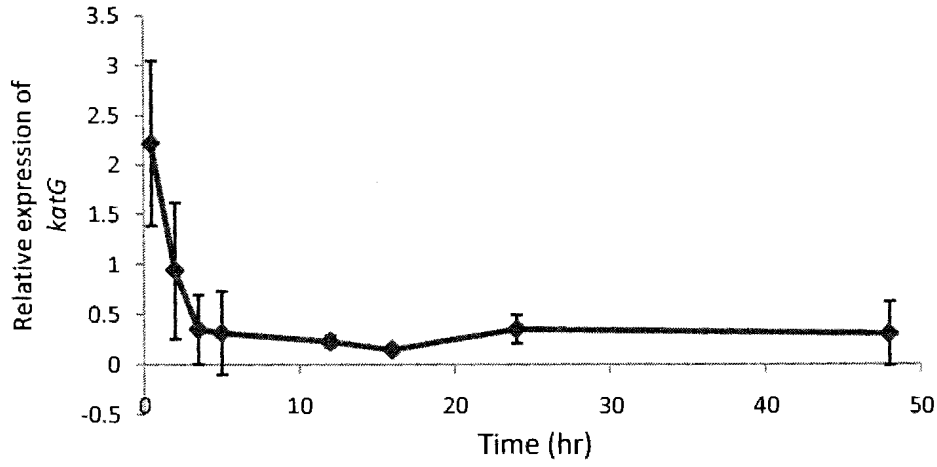

Figure 4.7: Inducibility of *katG* expression by 500 mg/L of nZVI

4.4. Summary

The effect of nZVI on different oxidative stress related mutants suggests that oxidative stress induced by ROS has an important role in the toxicity of nZVI on bacteria. *rpoS* contributes substantially to cell protection against nZVI, not only in stationary phase but also in other phases. The toxic effect of nZVI is mainly from superoxide generated inside cell membrane. Therefore, cell protection against nZVI is attributed to superoxide dismutase more than catalase. The repression of *katG* expression by nZVI was observed once bacterial cell entered exponential phase suggesting another mechanism contributing to cell inactivation.

CHAPTER 5. CONCLUSIONS AND RECOMMENDATIONS FOR FUTURE STUDIES

5. 1 Conclusions

In this study, the effect of bacterial growth phases on toxicity of nZVI and the contribution of oxidative stress to cell inactivation by the particles were investigated. Bacterial cells from different growth phases exhibited different level of susceptibility when exposed to nZVI. Cells in lag and stationary phases revealed less susceptibility to nZVI, whereas high and rapid inactivation was observed in exponential and declining phase cells. However, a statistic analysis suggested that only cells from stationary phase were significantly less susceptible to nZVI. Furthermore, the toxicity of these particles were both species and strain dependent since different levels of inactivation were observed among the two *E. coli* strains and the two *P. putida* strains studied. The level of toxicity of nZVI on bacteria was dose dependent; higher nZVI concentration inactivated more cells. Physical interaction between bacterial cells and nZVI was necessary for cell inactivation since only limited inactivation was detected when exposing cells to nZVI suspension filtrate.

The inactivation mechanism of nZVI on bacterial cells was further examined by exposing different oxidative stress related mutants to nZVI. Most of the mutants exhibited higher susceptibility to nZVI than the wildtype strain although a statistical analysis suggested that significantly higher susceptibility compared to the wildtype occurred only in the following strains: *rpoS*, *sodA*, and *sodB* mutants in lag and exponential phases, *rpoS* mutant in stationary phase, and *rpoS*, *sodA*, *sodB*, and *katE* mutants in declining phase. The higher susceptibility of these oxidative stress related mutants compared to the wildtype strain indicates that oxidative stress generated by nZVI contributes to bacterial cell

inactivation. Inactivation results of these mutants also suggested that superoxide produced by nZVI may be the major ROS responsible for cell inactivation, and this superoxide is mainly generated inside bacterial cells. Moreover, the inducibility of *katG* encoding for a defensive enzyme namely catalase was determined, and data revealed that, expression of *katG* was suppressed rather than induced once bacteria reached exponential phase. These data suggested that nZVI may correlate with certain genes repression.

5.2 Recommendations for Future Studies

The results obtained in this study provided more insight in how bacterial cells are inactivated by nZVI. However, in order to clearly understand the inactivation mechanism of these particles, more studies should be conducted including the investigation of global gene expression. This will provide useful knowledge about genes that are influenced by nZVI, and will also reveal whether gene suppression by nZVI is a general incident or occurs only to certain genes. Since the significance of physical contact between bacterial cells and nZVI in cell inactivation was confirmed in this study, experiments focusing on the interaction between them should be conducted including determination of cell membrane integrity and its ability in transporting substances across cell membrane after nZVI exposure. Moreover, the susceptibility of bacterial cells grown under stressful conditions (pH, heat, and osmolarity) to nZVI should also be investigated since most of the indigenous microbes in the environment are growing in stress conditions. Finally, the toxicity of nZVI on Gram positive bacteria at different growth phases should also be determined.

REFERENCES

Alexeeva, S., de Kort, B., Sawers, G., Hellingwerf, K. J., and de Mattos, M. J. T. Effects of Limited Aeration and of the arcAB System on Intermediary Pyruvate Catabolism in *Escherichia coli*. Journal of Bacteriology 182,17 (2000): 4934-4940.

Auffan, M. l., Achouak, W., Rose, J., Roncato, M. A., Chaneac, C., Waite, D. T., Masion, A., Woicik, A. C. Wiesner, M. R., and Bottero, J. Y. Relation between the Redox State of Iron-Based Nanoparticles and Their Cytotoxicity toward *Escherichia coli*. Environmental Science & Technology 42,17 (2008): 6730-6735.

Barnes, R. J., et al. The Impact of Zero-Valent Iron Nanoparticles on a River Water Bacterial Community. Journal of Hazardous Materials 184,1-3 (2010): 73-80.

Bortolussi, R., Vandenbroucke-Grauls, C. M., van Asbeck, B. S., and Verhoef, J. Relationship of Bacterial Growth Phase to Killing of *Listeria monocytogenes* by Oxidative Agents Generated by Neutrophils and Enzyme Systems. Infectious Immunology. 55,12 (1987): 3197-3203.

Chang, M. C., and Kang, H. Y. Remediation of Pyrene-Contaminated Soil by Synthesized Nanoscale Zero-Valent Iron Particles. Journal of Environmental Science and Health, Part A: Toxic/Hazardous Substances and Environmental Engineering 44,6 (2009): 576 - 582.

Christman, M. F., Morgan, R. W., Jacobson, F. S., and Ames, B. N. Positive Control of a Regulon for Defenses against Oxidative Stress and Some Heat-Shock Proteins in *Salmonella* Typhimurium. Cell 41,3 (1985): 753-762.

Davis, M. J., Coote, P. J., and O'Byrne, C. P. Acid Tolerance in *Listeria monocytogenes*: The Adaptive Acid Tolerance Response (ATR) and Growth-Phase-Dependent Acid Resistance. Microbiology 142,10 (1996): 2975-2982.

Demple, B. Redox Signaling and Gene Control in the *Escherichia coli soxRS* Oxidative Stress Regulon -- a Review. Gene 179,1 (1996): 53-57.

Demple, B. Regulation of Bacterial Oxidative Stress Genes. Annual Review of Genetics 25 (1991): 315-337.

Diao, M., and Yao, M. Use of Zero-Valent Iron Nanoparticles in Inactivating Microbes. Water Research 43,20 (2009): 5243-5251.

Dong, T., Kirchhof, M., and Schellhorn, H. RpoS Regulation of Gene Expression During Exponential Growth of ≪I≫Escherichia Coli≪/I≫ K12. Molecular Genetics and Genomics 279,3 (2008): 267-277.

Eisenstark, A., Calcutt, M. J., Becker-Hapak, M., and Ivanova, A. Role of *Escherichia coli* RpoS and Associated Genes in Defense against Oxidative Damage. Free Radical Biology and Medicine 21,7 (1996): 975-993.

Escolar, L., Perez-Martin, J., and de Lorenzo, V. Opening the Iron Box: Transcriptional Metalloregulation by the Fur Protein. Journal of Bacteriology 181,20 (1999): 6223-6229.

Escolar, L., Pérez-Martín, J., and de Lorenzo, V. Binding of the Fur (Ferric Uptake Regulator) Repressor of *Escherichia coli* to Arrays of the Gataat Sequence. Journal of Molecular Biology 283,3 (1998): 537-547.

Fee, J. A. Regulation of *sod* Genes in *Escherichia coli*: Relevance to Superoxide Dismutase Function. Molecular Microbiology 5,11 (1991): 2599-2610.

Gaudu, P., and Weiss, B. SoxR, a [2Fe-2S] Transcription Factor, is Active Only in Its Oxidized Form. Proceedings of the National Academy of Sciences of the United States of America 93,19 (1996): 10094-10098.

Gonzalez-Flecha, B., and Demple, B. Homeostatic Regulation of Intracellular Hydrogen Peroxide Concentration in Aerobically Growing *Escherichia coli*. Journal of Bacteriology 179,2 (1997): 382-388.

González-Flecha, B., and Demple, B. Metabolic Sources of Hydrogen Peroxide in Aerobically Growing *Escherichia coli*. Journal of Biological Chemistry 270,23 (1995): 13681-13687.

Gort, A. S., Ferber, D. M., and Imlay, J. A. The Regulation and Role of the Periplasmic Copper, Zinc Superoxide Dismutase of *Escherichia coli*. Molecular Microbiology 32,1 (1999): 179-191.

Gort, A. S., and Imlay, J. A. Balance between Endogenous Superoxide Stress and Antioxidant Defenses. Journal of Bacteriology 180,6 (1998): 1402-1410.

Greenberg, J. T., and Demple, B. A Global Response Induced in *Escherichia coli* by Redox-Cycling Agents Overlaps with That Induced by Peroxide Stress. Journal of Bacteriology 171,7 (1989): 3933-3939.

Grieger, K. D., Fjordboge, A., Hartmann, N. B., Eriksson, E.,Bjerg, B. L., and Baun, A. Environmental Benefits and Risks of Zero-Valent Iron Nanoparticles (NZVI) for in Situ Remediation: Risk Mitigation or Trade-Off? Journal of Contaminant Hydrology 118,3-4 (2010): 165-183.

Hengge, R. Proteolysis of [Sigma]S (RpoS) and the General Stress Response in *Escherichia coli*. Research in Microbiology 160,9 (2009): 667-676.

Hidalgo, E., and Demple, B. An Iron-Sulfur Center Essential for Transcriptional Activation by the Redox-Sensing Soxr Protein. The EMBO journal 13,1 (1994): 138-146.

Hidalgo, E., and Demple, B. Spacing of Promoter Elements Regulates the Basal Expression of the Soxs Gene and Converts SoxR from a Transcriptional Activator into a Repressor. EMBO Journal. 16,5 (1997): 1056-1065.

Hogg, S., ed. Essential Microbiology. John Wiley & Sons Ltd, 2005.

Huber, D. L. Synthesis, Properties, and Applications of Iron Nanoparticles. Small 1,5 (2005): 482-501.

Ishihama, A. Adaptation of Gene Expression in Stationary Phase Bacteria. Current Opinion in Genetics & Development 7,5 (1997): 582-588.

Iuchi, S., and Weiner, L. Cellular and Molecular Physiology of *Escherichia coli* in the Adaptation to Aerobic Environments. Journal of Biochemistry 120,6 (1996): 1055-1063.

Keenan, C. R., Goth-Goldstein, R., Lucas, D., and Sedlak, D. L. Oxidative Stress Induced by Zero-Valent Iron Nanoparticles and Fe(II) in Human Bronchial Epithelial Cells. Environmental Science & Technology 43,12 (2009): 4555-4560.

Kim, K. S., and Anthony, B. F. Importance of Bacterial Growth Phase in Determining Minimal Bactericidal Concentrations of Penicillin and Methicillin. Antimicrobial Agents Chemotherapy 19,6 (1981): 1075-1077.

Kim, S. O., et al. OxyR: A Molecular Code for Redox-Related Signaling. Cell 109,3 (2002): 383-396.

Korshunov, S. S., and Imlay, J. A. A Potential Role for Periplasmic Superoxide Dismutase in Blocking the Penetration of External Superoxide into the Cytosol of Gram-Negative Bacteria. Molecular Microbiology 43,1 (2002): 95-106.

Lee, C., Kim, J. Y., Lee, W. I., Nelson, K. L., Yoon, J., and Sedlak, D. L. Bactericidal Effect of Zero-Valent Iron Nanoparticles on *Escherichia coli*. Environmental Science & Technology 42,13 (2008): 4927-4933.

Lee, I. S., Slonczewski, J. L., and Foster, J. W. A Low-pH-Inducible, Stationary-Phase Acid Tolerance Response in *Salmonella* Typhimurium. Journal of Bacteriology 176,5 (1994): 1422-1426.

Li, X.-q., Elliott, D. W., and Zhang, W.-x. Zero-Valent Iron Nanoparticles for Abatement of Environmental Pollutants: Materials and Engineering Aspects. Critical Reviews in Solid State and Materials Sciences 31,4 (2006): 111 - 122.

Liu, Y., Majetich, S. A., Tilton, R. D., Sholl, D. S., and Lowry, G. V. TCE Dechlorination Rates, Pathways, and Efficiency of Nanoscale Iron Particles with Different Properties. Environmental Science & Technology 39,5 (2005): 1338-1345.

Loewen, P. C., and Triggs, B. L. Genetic Mapping of *katF*, a Locus That with *katE* Affects the Synthesis of a Second Catalase Species in *Escherichia coli*. Journal of Bacteriology 160,2 (1984): 668-675.

Loui, C., Chang, A., and Lu, S. Role of the Arcab Two-Component System in the Resistance of *Escherichia coli* to Reactive Oxygen Stress. BMC Microbiology 9,1 (2009): 183.

Lushchak, V. I. Adaptive Response to Oxidative Stress: Bacteria, Fungi, Plants and Animals. Comparative Biochemistry and Physiology Part C: Toxicology & Pharmacology 153,2 (2011): 175-190.

Lushchak, V. I. Oxidative Stress and Mechanisms of Protection against It in Bacteria. Biochemistry (Moscow) 66,5 (2001): 476-489.

Lynch, M., and Kuramitsu, H. Expression and Role of Superoxide Dismutases (SOD) in Pathogenic Bacteria. Microbes and Infection 2,10 (2000): 1245-1255.

Michan, C., Manchado, M., Dorado, G., and Pueyo, C. In Vivo Transcription of the *Escherichia coli oxyR* Regulon as a Function of Growth Phase and in Response to Oxidative Stress. Journal of Bacteriology 181,9 (1999): 2759-2764.

Miksch, G., and Dobrowolski, P. Growth Phase-Dependent Induction of Stationary-Phase Promoters of *Escherichia coli* in Different Gram-Negative Bacteria. Journal of Bacteriology 177,18 (1995): 5374-5378.

Nel, A., Xia, T., Mädler, L., and Li, N. Toxic Potential of Materials at the Nanolevel. Science 311,5761 (2006): 622-627.

Niederhoffer, E. C., Naranjo, C. M., Bradley, K. L., and Fee, J. A. Control of *Escherichia coli* Superoxide Dismutase (sodA and sodB) Genes by the Ferric Uptake Regulation (Fur) Locus. Journal of Bacteriology 172,4 (1990): 1930-1938.

Nunoshiba, T., Hidalgo, E., Amabile Cuevas, C. F., and Demple, B. Two-Stage Control of an Oxidative Stress Regulon: The *Escherichia coli* SoxR Protein Triggers Redox-Inducible Expression of the Soxs Regulatory Gene. Journal of Bacteriology 174,19 (1992): 6054-6060.

Nurmi, J. T., Tratnyek, P. G., Saranthy, V., Baer, D. R., Amonette, J. E., Pecher, K., Wang, C., Linehan, J. C., Matson, D. W., Penn, R. L., and Driessen, M. D. Characterization and Properties of Metallic Iron Nanoparticles: Spectroscopy, Electrochemistry, and Kinetics. Environmental Science & Technology 39,5 (2004): 1221-1230.

Phenrat, T., Saleh, N., Sirk, K., Tilton, R. D., and Lowry, G. V. Aggregation and Sedimentation of Aqueous Nanoscale Zerovalent Iron Dispersions. Environmental Science & Technology 41,1 (2006): 284-290.

Pomposiello, P. J., and Demple, B. Redox-Operated Genetic Switches: The SoxR and OxyR Transcription Factors. Trends in Biotechnology 19,3 (2001): 109-114.

Quinn, J., Geiger, C., Clausen, C., Coon, C., Ohara, S., Krug, T., Major, D., Yoon, W. S., Gavaska, A., and Holdsworth, T. Field Demonstration of DNAPL Dehalogenation Using Emulsified Zero-Valent Iron. Environmental Science & Technology 39,5 (2005): 1309-1318.

Rahman, M., Hasan, M., and Shimizu, K. Growth Phase-Dependent Changes in the Expression of Global Regulatory Genes and Associated Metabolic Pathways in *Escherichia coli*. Biotechnology Letters 30,5 (2008): 853-860.

Schellhorn, H. E. Regulation of Hydroperoxidase (Catalase) Expression in *Escherichia coli*. FEMS Microbiology Letters 131,2 (1995): 113-119.

Schellhorn, H. E., and Hassan, H. M. Transcriptional Regulation of katG in *Escherichia coli* K-12. Journal of Bacteriology 170,9 (1988): 4286-4292.

Schrick, B., Hydutsky, B. W., Blough, J. L., and Mallouk, T. E. Delivery Vehicles for Zerovalent Metal Nanoparticles in Soil and Groundwater. Chemistry of Materials 16,11 (2004): 2187-2193.

Schweder, T., Lee, K., Lomovskaya, O., and Matin, A. Regulation of *Escherichia coli* Starvation Sigma Factor (Sigma S) by Clpxp Protease. Journal of Bacteriology 178,2 (1996): 470-476.

Signorini, L., et al. Size-Dependent Oxidation in Iron/Iron Oxide Core-Shell Nanoparticles. Physical Review B 68,19 (2003): 195423.

Small, P., Blankenhorn, D., Welty, D., Zinser, E., and Slonczewski, J. L. Acid and Base Resistance in *Escherichia coli* and *Shigella flexneri*: Role of RpoS and Growth pH. Journal of Bacteriology 176,6 (1994): 1729-1737.

Stevens, D. L., Van, S., and Bryant, A. E. Penicillin-Binding Protein Expression at Different Growth Stages Determines Penicillin Efficacy in Vitro and in Vivo: An Explanation for the Inoculum Effect. Journal of Infectious Diseases 167,6 (1993): 1401-1405.

Storz, G., Tartaglia, L. A., and Ames, B. N. The *oxyR* Regulon. Antonie van Leeuwenhoek 58,3 (1990): 157-161.

Storz, G., Tartaglia, L. A., Farr, S. B., and Ames, B. N. Bacterial Defenses against Oxidative Stress. Trends in Genetics 6 (1990): 363-368.

Su, H. L., Chou, C. C., Hung, D. J., Lin, S. H., Huang, F. L., Dong, R. X., and Lin, J. J. The Disruption of Bacterial Membrane Integrity through ROS Generation Induced by Nanohybrids of Silver and Clay. Biomaterials 30,30 (2009): 5979-5987.

Sun, Y.-P., Li, X.-q., Cao, J., Zhang, W.-x., and Wang, H. P. Characterization of Zero-Valent Iron Nanoparticles. Advances in Colloid and Interface Science 120,1-3 (2006): 47-56.

Talukder, A. A., Yanai, S., Nitta, T., Kato, A., and Yamada, M. RpoS-Dependent Regulation of Genes Expressed at Late Stationary Phase in *Escherichia coli*. FEBS Letters 386,2-3 (1996): 177-180.

Tanaka, K., Handel, K., Loewen, P. C., and Takahashi, H. Identification and Analysis of the RpoS-Dependent Promoter of Kate, Encoding Catalase HPII in *Escherichia coli*. Biochimica et Biophysica Acta (BBA) - Gene Structure and Expression 1352,2 (1997): 161-166.

Tardat, B., and Touati, D. Two Global Regulators Repress the Anaerobic Expression of MnSOD in *Escherichia coli*: Fur (Ferric Uptake Regulation) and Arc (Aerobic Respiration Control). Molecular Microbiology 5,2 (1991): 455-465.

Theron, J., Walker, J. A., and Cloete, T. E. Nanotechnology and Water Treatment: Applications and Emerging Opportunities. Critical Reviews in Microbiology 34,1 (2008): 43-69.

Touati, D. Iron and Oxidative Stress in Bacteria. Archives of Biochemistry and Biophysics 373,1 (2000): 1-6.

Triggs-Raine, B. L., and Loewen, P. C. Physical Characterization of katG, Encoding Catalase HPI of *Escherichia coli*. Gene 52,2-3 (1987): 121-128.

Valko, M., Izakovic, M., Mazur, M., Rhodes, C. J., and Telser, J. Role of Oxygen Radicals in DNA Damage and Cancer Incidence. Molecular and Cellular Biochemistry 266,1 (2004): 37-56.

Vattanaviboon, P., and Mongkolsuk, S. Unusual Adaptive, Cross Protection Responses and Growth Phase Resistance against Peroxide Killing in a Bacterial Shrimp Pathogen, Vibrio Harveyi. FEMS Microbiology Letters 200,1 (2001): 111-116.

Wang, C.-B., and Zhang, W.-x. Synthesizing Nanoscale Iron Particles for Rapid and Complete Dechlorination of Tce and Pcbs. Environmental Science & Technology 31,7 (1997): 2154-2156.

White, D., ed. The Physiology and Biochemistry of Prokaryotes. Third ed: Oxford University Press, 2007.

Zhang, W.-x. Nanoscale Iron Particles for Environmental Remediation: An Overview. Journal of Nanoparticle Research 5,3 (2003): 323-332.

Zhang, W.-x., and Elliott, D. W. Applications of Iron Nanoparticles for Groundwater Remediation. Remediation Journal 16,2 (2006): 7-21.